ROS function as a distinct mitochondrial retrograde response factor for appropriate cardiogenic specifications and cardiac function in Drosophila embryos

Swati Sharma*[1]

*Molecular Cell and Developmental Biology Laboratory, Department of Biological Sciences, Indian Institute of Science Education and Research (IISER), Mohali 140306, India

ORCID ID: 0000-0002-7811-3158

Corresponding Author: Swati Sharma, Indian Institute of Science Education and Research, Mohali, 4L1, Academic Block 1, Knowledge City, Sector-81, Mohali, Punjab, 140306, Punjab, India. E mail: swatisharma@iisermohali.ac.in

Abstract:

Congenital Heart Diseases (CHDs) are major cause of prenatal and neonatal mortality. These defects occur due to abnormalities during heart formation in utero. The treatments of CHDs pose a major challenge due to lack of in depth understanding of underlying factors. There are certain evidences that suggest abnormal mitochondrial function in these cardiomyopathies. A large percentage of prenatal dilated cardiomyopathies reportedly exhibit defects in mitochondrial oxidative phosphorylation. However, we still have a very little understanding of causal role played by mitochondria in CHDs. Considering the fact that heart has highest density of mitochondria followed by skeletal muscles and central nervous system, investigation of mitochondrial involvement in CHDs is a very intriguing question.

The *Drosophila* embryonic heart is termed as dorsal vessel. It is a simple contractile tube which is similar to the tubular heart of early vertebrate embryo. Despite the evolutionary distance between *Drosophila* and vertebrates, cardio genesis is governed by similar fundamental mechanisms. The transcription factors as well as signalling pathways involved in cardio genesis are highly conserved among *Drosophila* and vertebrates. Dorsal vessel is comprised of merely104 cardio blasts; an extremely simple organ; hence enables pinpointing any minor cardiac deformity. The anterior portion is termed aorta whereas posterior portion is termed Heart proper. Hemolymph flows from posterior to anterior of the dorsal vessel. The posterior portion has specific subset of cardio blasts that form the inflow tracts termed as Ostia. Dorsal vessel has segmental repeated pattern of cell types which is a hallmark of insects. The cardio blasts are flanked by pericardial cells which function as nephrocytes. *Drosophila* can prove to be a good

model system to understand cardiac development and function, which can open new doors to understand cardiomyopathies and improve their treatment.

In order to perturb mitochondrial complex-I activity during embryonic development, two components of complex-I of ETC; *ND75* which is the largest core subunit of complex-I and *ND42*, an accessory subunit required for the assembly of complex-I of ETC were knocked down at different temporal and spatial windows and embryos were observed for lethality in terms of hatching rate. Severe embryonic lethality was observed in F1 progeny embryos by knocking down *ND42* and *ND75* with *Twist* Gal4. *Twist Gal4* is the early mesoderm Gal4 driver. Its expression starts at stage 4 when mesoderm begins to form. Live imaging of these embryos indicate cardiac malfunction at stage 17 of embryonic development. Quantitative analysis of cardiac parameters using SOHA (Semi-automated Heartbeat Analysis) confirmed the cardiac defects with respect to different parameters for example Heart rate, Heart period, systole-diastole diameters and systole -diastole intervals.

Further investigation of the cardiac defect in knock down embryos at cellular level revealed an intriguing cell specification defect at stage 16 of embryonic development. In wild type stage 16 embryo, cardiac tube is formed of 4 *Tinman* positive and 2 *Seven up* positive cardio blasts in each hemi segment. However, in complex-I mutant embryos, we found that this 4+2 pattern of cardio blasts is altered to 2+4 pattern. By tracking this phenotype to the earlier stages, we found that this change in cell identity initiates at stage 13 where some of *Tinman* positive cells begin to lose *Tinman* expression and ectopically begins to express *Seven up*. Therefore, ***identity of cells is changed due to metabolic disturbances***. In the complex-I knockdown embryos, ROS levels were found to be high as indicated by mitoSOX dye and *gstD GFP* reporter line. Co-immunostaining of *Twist* protein and *gst* D GFP showed that ROS levels were only increased in the *Twist* expressing mesoderm cells at stage 10 of embryonic development, suggesting that knockdown of *ND42/ND75* using *Twist Gal4* has resulted in elevated ROS levels in mesodermal population. We were able to establish ROS as the key mediator to elicit retrograde response from mitochondria to regulate cell fate specification since over-expression of SOD2 in the background of *ND42/ND75* knockdown was able to significantly rescue embryonic lethality, cardiac malfunctioning and cell fate specification defects.

Introduction

Congenital heart defects (CHD) are structural and functional abnormalities in heart structure that occur before birth. Approximately 8 out of 1000 newborns have CHDs ranging from mild to severe (Chen et al., 2018, Gilboa et al., 2016, Hoffman and Kaplan, 2002). Congenital heart defects occur due to incomplete or abnormal development of fetus heart during the early weeks of pregnancy (Peterson et al., 2014). Some CHDs are known to be associated with genetic disorders such as Down syndrome (Benhaourech et al., 2016). However, the cause of most of them is unknown. Investigating the mechanism by which these abnormalities happen during early embryonic development might have an impact on clinical management of these congenital malformations.

There are certain metabolic factors that are known to increase the risk of having CHDs; however, no obvious cause is identified in most cases (Verkleij-Hagoort et al., 2006, Wang et al., 2013, Brandalize et al., 2009). The primary congenital cardiomyopathies occur commonly in the cardiac muscle, with abnormal cardiac metabolism apparent soon after birth or early infancy (Wenink and Gittenberger-de Groot, 2005). Abnormalities (mutations/ knock out/ failed transcription) of mitochondrial DNA and/or nuclear genes encoding proteins involved in mitochondrial oxidative phosphorylation are also evident in cardiomyopathies (Giordano, 2005). Particularly, complex-I, III and IV of Electron Transport Chain present on the inner membrane of mitochondria are reported to be involved in various cardiomyopathies (Scheubel et al., 2002). Mutations of two nuclear genes *NDUFV2* and *NDUFS2* encoding complex-I subunits have been strongly linked with early onset hypertrophic cardiomyopathies. These mutations caused a marked decrease in the amount of nuclear-encoded subunits and complex-I activity (Benit et al., 2003). Mutation in *NDUFV2* has also been linked to Parkinson's disease, an association that may illustrate the large variety of clinical expression of mitochondrial disorders (Nishioka et al., 2010).

There are accumulating pieces of evidence that suggest that mitochondrial dysfunction plays a key role in early cardiac defects (Neubauer, 2007). There are reports which suggest that impairment of mitochondrial DNA replication and mitochondrial DNA deletion precedes heart failure in children with CHDs (Marin-Garcia et al., 1997). Based on these reports, the relationship between mitochondrial biogenesis and risks of CHDs are indicated (Karamanlidis et

al., 2010). There is a need to develop a model system for in depth analysis of mitochondrial associated CHDs.

In the current study, *Drosophila* embryonic heart is established as a model system to study CHDs so that an association between metabolic dysfunction and CHDs can be questioned on the cellular level. *Drosophila* embryonic heart has emerged as one of the most attractive model systems to study cardiac defects due to its simplicity and easy genetic manipulations (Piazza and Wessells, 2011). Additionally, most of the transcription factors and signaling pathways involved in cardiogenesis are highly conserved in *Drosophila* and vertebrates despite their evolutionary distance making the fly research highly relevant to human cardiac pathologies (Tao and Schulz, 2007, Medioni et al., 2008).

RESULTS:

Knocking down genes encoding complex-I components of ETC from the developing mesoderm leads to embryonic lethality in *Drosophila*

By knocking down genes encoding complex-I components *ND42* and *ND75* from the developing mesoderm using various Gal4 drivers that drive dsRNA mediated knockdown in a distinct spatiotemporal manner, it was found that relatively late embryonic stage Gal4 drivers were not able to induce any lethality in terms of hatching rate of embryos (Fig.1B) whereas *Twist*Gal4 induced early mesoderm knockdown of *ND42* and *ND75* leads to severe decline in hatching rate of the embryos (Fig.1B).

In the synchronized collection batches of *Twist Gal4*/+; *UAS GFP RNAi*/+ genotype, average 87 percent embryos were hatched, whereas in *TwistGal4/+;UASND42RNAi/+* and *TwistGal4/+;UAS ND75RNAi/+*, only 20% and 21% embryos were hatched respectively ($p<0.0001$) (Fig.1B). These result infer that by knocking down complex-I components using *TwistGal4* as a driver, there is a drastic reduction in hatching rate of embryos. For the lethality assay, *UAS ND42RNAi* and *UAS ND75RNAi* lines from BDSC and VDRC were assayed, which showed similar lethality trends in F1 progeny (Fig.S1).

The remaining 80 percent unhatched embryos were followed for the next 24 hours confirming there was no late hatching and all of them were non-viable (unpublished data).

From these results, it was clear that knock-down of complex-I encoding components by using very early driver *TwistGal4* was detrimental to the survivability of embryos to a significant level.

By knocking down *ND42* and *ND75* using *DaughterlessGal4 (DaGal4)* which is a ubiquitous Gal4 driver, it was found that complex-I activity is declined to significant levels. In case of *DaGal4/+; UAS ND42RNAi/+*, an average of 66% complex-I activity is left whereas in case of *DaGal4/+;UAS ND75RNAi/+*, an average of 40% activity is left (Fig.1C). qRT PCR analysis revealed a drastic decline in fold change transcript levels of *ND42* and *ND75* in case of *DaGal4/+;UAS ND42RNAi/+* and *DaGal4/+;UAS ND75RNAi/+* knockdown embryos respectively(Fig.1D).

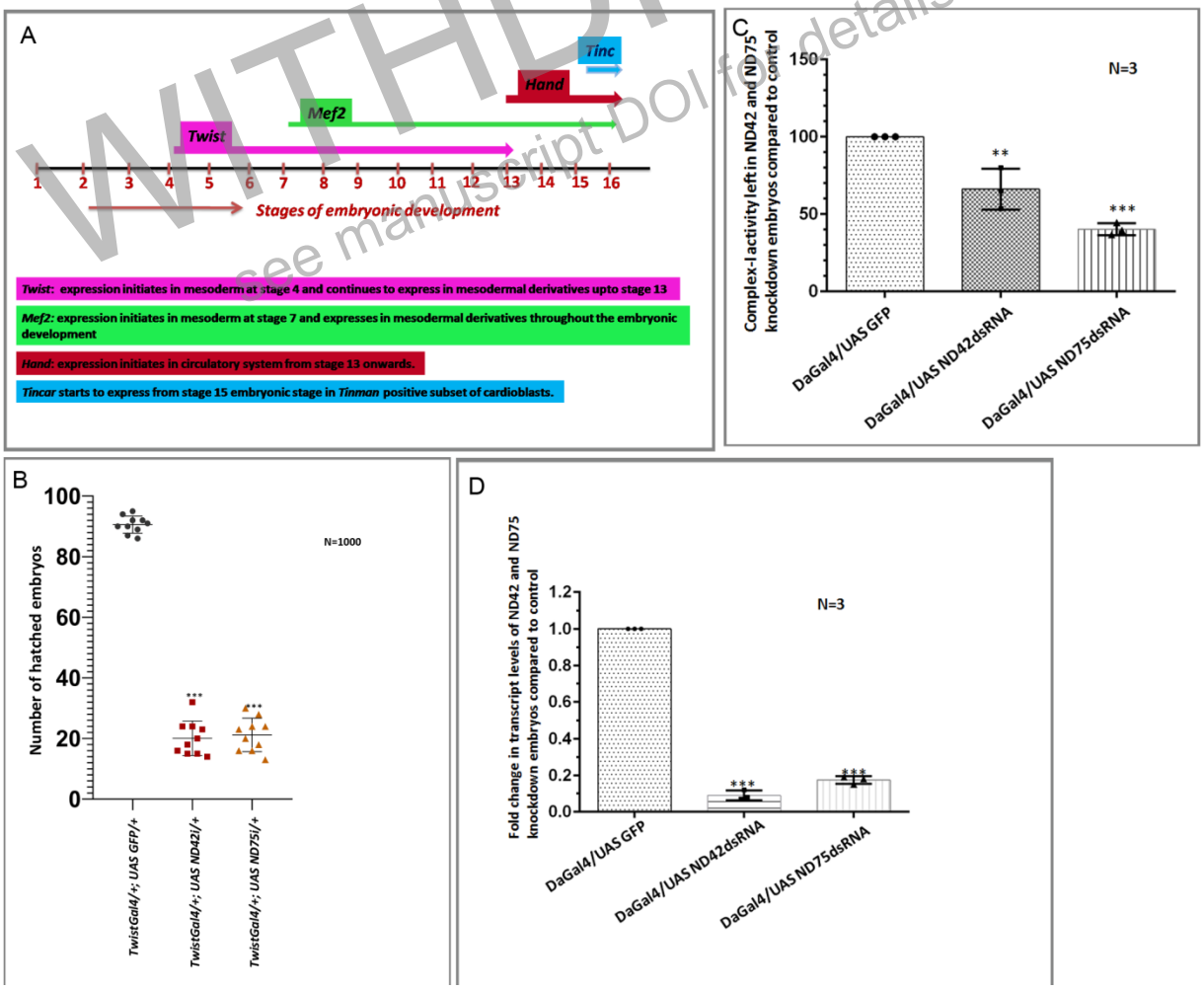

Figure 1: Knockdown of *ND42* and *ND75* from the developing mesoderm using *Twist*Gal4 imparts severe embryonic lethality. Schematic representation of spatiotemporal expression profile of four Gal4 drivers.used to knock down *ND42* and *ND75* from the developing mesoderm. *Hand* and *Tincar* are relatively late Gal4 drivers whereas *Mef2* and *Twist* expression initiates very early **(A).** Statistical analysis of hatching rate of embryos (in UAS *GFP*, UAS *ND42* RNAi and UAS *ND75* RNAi backgrounds using 4 different Gal4 drivers) showing no significant change in hatching rate with *tin car delta4* gal4, *Hand* Gal4 and *Mef2* Gal4 whereas around 80 percent reduction in hatching rate with *TwistGal4* compared to control (n=1000) **(B).** The decline in Complex-I activity by knocking down *ND42* and *ND75* using *Da*Gal4 in larvae **(C).** qRT PCR showing fold change in transcript levels of *ND42* and *ND75* compared to control by knocking down these complex-I components using *Da*Gal4 in stage 16 embryos **(D**).

Dorsal vessel is severely affected in terms of functionality in complex I knockdown embryos

Live imaging of stage 17 *Drosophila* embryonic hearts was done and heartbeat was quantitatively analyzed using SOHA (Semi-automated Heartbeat Analysis) software (Ocorr et al., 2009).

M-mode represents the vertical movement of heart tube edges (y-axis) over time (x-axis)

We used the heart proper region in the cardiac tube of stage 17 *Drosophila* embryos to generate M-mode since the beating originates in the heart proper region and then propagates through the rest of the tube. M-modes were made from the same region of the cardiac tube in control and knockdown embryos.

A) Wild type M-mode shows regular heart contractions (Fig.2H) as evidenced by periodic movement of heart edges along time (Movie 1).
B) *ND42* and *ND75* knockdown embryos show aberrations in their M-modes (Fig.2I, 2J), primarily characterized by prolonged relaxations and very rare and less robust contractions as clearly evident in the live imaging videos of ND42 knockdown embryos a (Movie 2) and ND75 knockdown embryos (Movie 3).

Increase in the heart period of stage 17 wild type, ND42, and ND75 knockdown embryos.

Heart period is measured as the interval between the start of one diastole and the beginning of the next. The heart period is significantly increased in both *ND42* and *ND75* knockdown embryos compared to control. The heart period of *Hand* GFP; *TwistGal4/+; UAS ND42 RNA*i/+ embryos is 3.2 millisecond (ms) compared to the heart period of 1.2 ms in control (Fig.2C). The

heart period of *Hand* GFP*;TwistGal4/+;UAS ND75RNAi/+* knockdown embryos is increased to 3.1 ms (*P=0.000103 and 0.00058 respectively for *ND42* and *ND75* knockdown embryos, by t-test) (Fig. 2C) Data are mean +_ SE. Increase in heart period indicates prolonged systole-diastolic phase i.e. heart spends more time to complete one systole-diastole cycle compared to the control.

Diastolic interval is increased in ND42 and ND75 knockdown embryos

Diastolic interval (DI) is the duration for which the heart stays in the diastolic (relaxation) phase. The diastolic interval of *ND42* knockdown embryos was 3.1 millisecond compared to 0.6 ms in control (*P= 5.15E-05 by t-test). In the case of *ND75* knockdown embryos, the diastolic interval was increased to 2.8 ms (*P= 0.000121 by t-test) (Fig.2A). Increased diastolic interval indicates heart remains in relaxation phase for a longer time in case of *ND42* and *ND75* knockdown embryos compared to control.

Systolic interval was reduced in ND42 and ND75 knockdown embryos

Systolic interval (SI) is the duration for which cardiac tube stays in the systolic (contraction) phase. The systolic interval of *ND42* knockdown embryos was decreased to 0.21 ms compared to the systolic interval of 0.6 ms in control embryos (*P= 3..26E-05, by t-test). In the case of *ND75* knockdown embryos, the systolic interval was reduced to 0.22 ms (*P= 4.41-E06, by t-test) (Fig.2B). Reduction in systolic interval suggests that heart contraction phase is shorter in knockdown embryos compared to control.

ND42 and ND75 Knockdown embryo exhibit significantly reduced diastolic diameter

The diastolic diameter of *ND42* knockdown embryos was 43.73 microns compared to 95.52 microns in control (*P= 9.08E-10) whereas the diastolic diameter of *ND75* knockdown embryos was significantly reduced to 45.19 microns (*P=3.84E-10) (Fig.2E).

Reduced systole diameter in ND42 and ND75 knockdown embryos:

The systolic diameter of *ND42* knockdown embryos was significantly reduced to 27.77 microns compared to the systolic diameter of 66.38 microns in control whereas the systolic diameter of

ND75 knockdown embryos is reduced to 32.65 microns (*P =4.45E-08 and P= 3.12E-07 respectively in *ND42* and *ND75* knockdown embryos, by T-test) (Fig.2F).

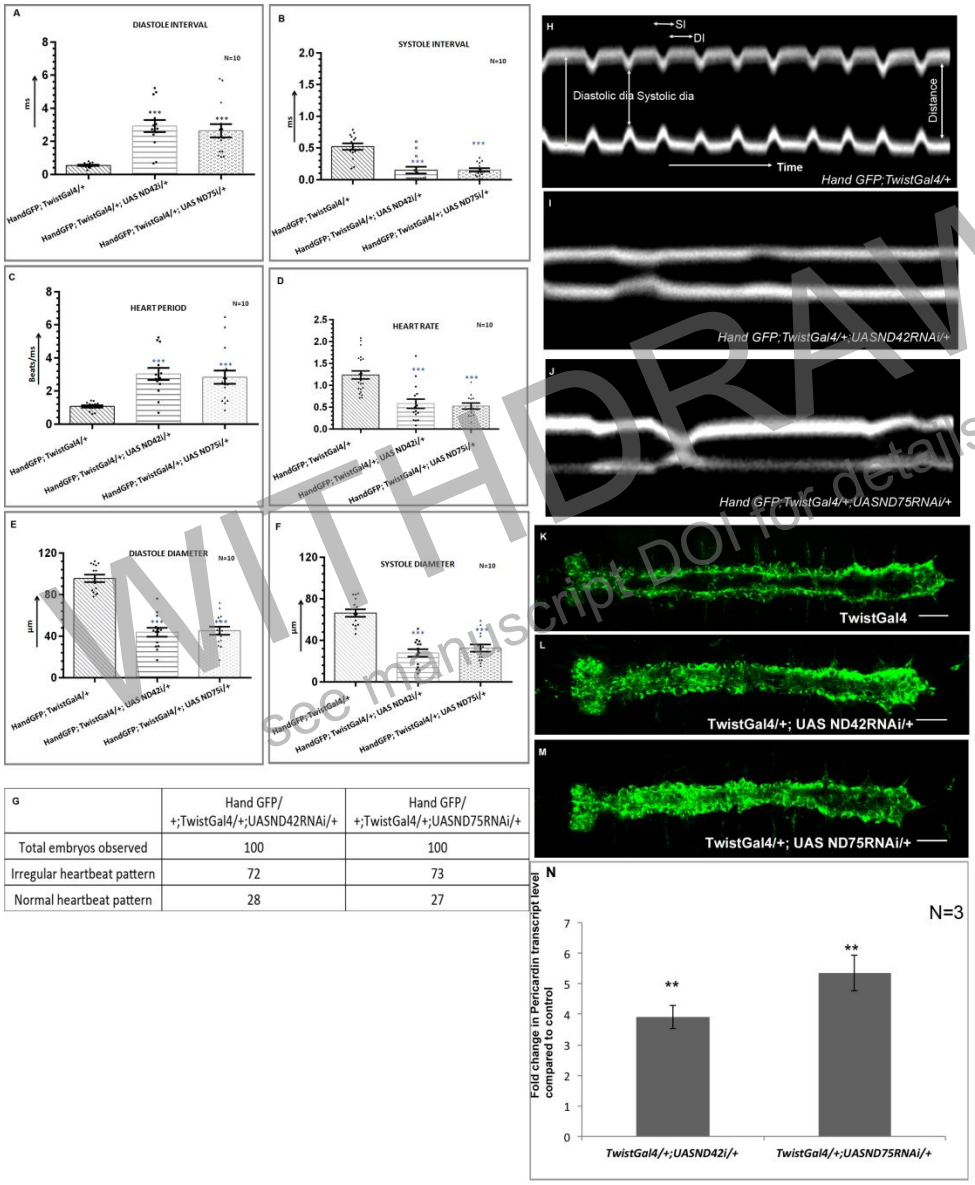

G	Hand GFP/ +;TwistGal4/+;UASND42RNAi/+	Hand GFP/ +;TwistGal4/+;UASND75RNAi/+
Total embryos observed	100	100
Irregular heartbeat pattern	72	73
Normal heartbeat pattern	28	27

Fig. 2 Knockdown of *ND42* and *ND75* from the developing mesoderm leads to structural and functional defects in embryos. Measurement of various cardiac parameters using SOHA (Semi-automated heartbeat analysis) shows an increase in diastole interval and decrease in systole interval in knockdown embryos compared to control **(A,B**) increase in heart period **(C)**, decrease in heart rate(**D)** and decrease in systole-diastole diameters (**E, F**) compared to control. Quantitative analysis of the number of embryos showing irregular heartbeat pattern vs normal heartbeat pattern (n=100) (**G**). M-mode representing movement of heart wall with respect to time shows a drastic

change in *ND42* **(I)** and *ND75* **(J)** knockdown embryos compared to regular M-mode pattern in control (**H)**. Wild type stage 16 embryo immunostained for *Pericardin* which is secreted by pericardial cells, marking boundaries of the cardiac tube **(K).** The increase in *Pericardin* expression can be seen along with its mislocalization in the lumen of *ND42* and *ND75* knockdown embryo at stage 16 of embryonic development **(L, M**). *Pericardin* transcript levels in stage 16 embryo are increased 4 fold and 5 fold in *ND42* and *ND75* knockdown embryos at stage 16 of embryonic development as revealed by qRT PCR (n=3) (**N)**. Scale bar: 20µm

Increased and mislocalized *Pericardin* in the lumen of the cardiac tube of *ND42 and ND75* knockdown embryos:

Pericardin is a type-IV collagen-like protein expressed by pericardial cells and a subpopulation of cardioblasts. It is concentrated at the basal surface of cardioblasts and around the pericardial cells in close proximity to the dorsal ectoderm and is absent from the lumen (Chartier et al., 2002). *Pericardin* marks the boundaries of the cardiac tube as well as alary muscles (Chartier et al., 2002). Interestingly, in *ND42* (Fig.2L) and *ND75* (Fig.2M) knockdown embryos, immunostaining with *Pericardin* antibody revealed an excessive *Pericardin* deposition around the cardiac tube compared to control embryos at stage 16 of embryonic development (Fig.2K). The *Pericardin* expression is mislocalized in the luminal region and seems to be diffused rather than concentrated around the pericardial cells in wild type embryos.

qRT PCR for *Pericardin* of stage 16 embryos revealed increased *Pericardin* transcript levels in *ND42* and *ND75* knockdown embryos. In the case of *ND42* knockdown embryos, the *Pericardin* transcript reportedly increased to 4 folds compared to control. In the case of *ND75* knockdown embryos, there were 5 fold changes in *Pericardin* transcript levels compared to the same stage control embryos (Fig.2N). These results established an increase in *Pericardin* transcript levels in *ND42* and *ND75* knockdown embryos. Although the question of whether there are any changes in the number of pericardial cells remained unanswered. Zfh1 marks all the pericardial cell populations as well as the lymph gland (Ward and Skeath, 2000). In order to precisely calculate pericardial subpopulations and to eliminate lymph gland cells, co-immunostaining with *Zfh1* and *Pericardin* was done since lymph gland cells do not express *Pericardin.* Quantitative analysis revealed no significant change in the total number of pericardial cells in *ND42* and *ND75* knockdown embryos compared to control (Fig.S4).

These two results suggest that increased *Pericardin* accumulation is the result of more *Pericardin* produced per pericardial cell instead of a change in the total number of pericardial cells.

Lumen constriction revealed by *Trol*GFP in complex-I knockdown embryos:

In order to ascertain the results mentioned in the previous result section which stated that systolic and diastolic diameters were reduced in *ND42*/*ND75* knockdown embryos (Fig.2E and 2F), *Trol GFP* was used as a marker to determine the status of the lumen of the cardiac tube at stage 16 of embryonic development.

Trol (Terribly Reduced Optic Lobes) is the heparin sulfate proteoglycan and the vertebrate protein *Perlecan* homolog in *D. melanogaster*. It is expressed in the basement membrane of embryonic tissues. In the dorsal vessel at stage 16 of embryonic development, it marks the lumen of the cardiac tube as well as the outer boundaries of the cardiac tube and alary muscles (Medioni et al., 2008).

Inner lumen diameter, as well as the outer diameter of the cardiac tube, was measured in the *TrolGFP* background in control and knockdown embryos. Statistical analysis was performed by taking 10 measurements at different points, each for aorta and heart proper region and then averaged to give a mean value for aorta and heart proper region.

Confocal imaging of *TrolGFP* marked *ND42* and *ND75* knockdown embryos indicates that the lumen of the cardiac tube is constricted in *ND42* knockdown embryos (Fig.3B, F and G) compared to control (Fig. 3.7A, D and E). A similar lumen constriction was observed in *ND75* knockdown embryos (Fig.3C, H and I).

Detailed quantitative analysis confirmed that the inner lumen is significantly constricted in *ND42* (Fig.3J) and *ND75* knockdown embryos (Fig. 3K) with *P value< 0.0001, by T-test. In control embryos at stage 16, the average lumen diameter in the Aorta region is 3.15 microns and in the Heart proper region, the lumen diameter is 3.29 microns. In *TrolGFP;TwistGal4/+; UAS ND42 RNA*i/+ knockdown embryos, aorta and heart proper lumen diameter is significantly reduced to 1.5 microns and 1.95 microns respectively. In *TrolGFP;TwistGal4/+;UAS ND75RNAi/+*

knockdown embryos, aorta and heart proper lumen diameter is significantly reduced to 1.55 microns and 1.93 microns respectively (Fig. 3J).

Quantitative analysis of the outer diameter of the cardiac tube revealed no significant change in knockdown embryos compared to control. In control embryos at stage 16 of embryonic development, the outer diameter in Aorta and Heart proper region is 11.36 microns and 15.97 microns respectively. In *ND42* knockdown embryos, outer lumen diameter in aorta region was measured 11.29 microns and in the heart proper region was measured as 15.71 microns with no significant change compared to control. In *TrolGFP;TwistGal4/+;UAS ND75RNAi/+*, aorta measures 10.8 microns and the heart proper region measures 15.26 microns, again no significant change compared to control (Fig. 3K).

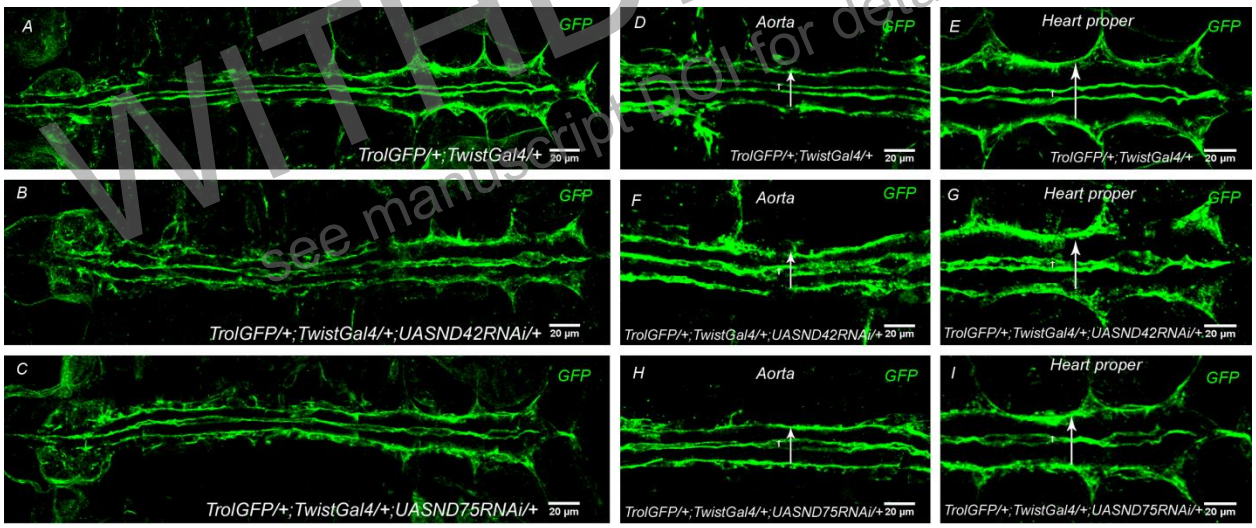

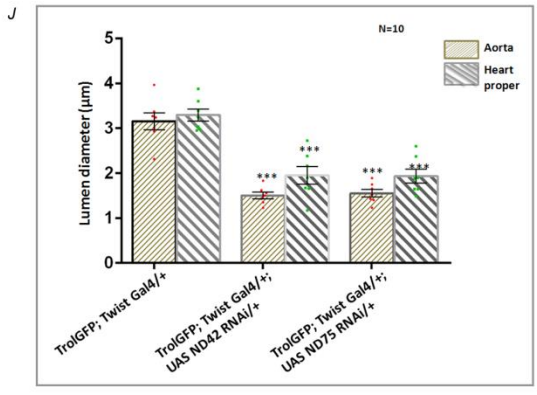

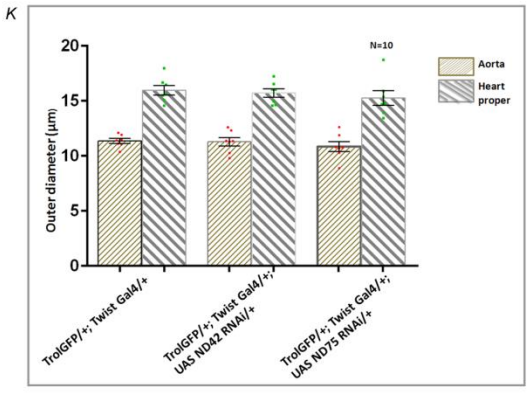

Fig. 3 Luminal constriction in *ND42* and *ND75* knockdown embryos. Wild type stage 16 embryos stained for *Trol*GFP which is present in the basement membrane and used to mark the lumen and outer wall of the cardiac tube **(A).** In *TwistGal4*/+; UAS *ND42* RNAi/+ and *Twist*Gal4/+; UAS *ND75* RNAi/+ knockdown embryos, the lumen is notably constricted compared to control in the cardiac tube **(B, C**). Zoomed in images of the same embryos shown on the left clarifying lumen constriction in *ND42* and *ND75* knockdown embryos in the aorta as well as heart proper regions (**D, I**). Statistical analysis showed a significant reduction in lumen diameter in knockdown embryos compared to control (n=10) **(J**) No significant change in outer diameter of the cardiac tube in knockdown embryos compared to the control **(K**). Scale bar: 20µm

Metabolic disturbances target cell fate decisions during cardiogenic mesoderm specifications

In wild type embryos at stage 16 of embryonic development, the cardiac tube has a 4+2 pattern of cardioblasts in each hemisegment (4 *Tinman* positive cardioblasts+2 *Seven up* positive cardioblasts) as reported previously (Gajewski et al., 2000, Lo and Frasch, 2001) and evident from co-immunostaining for *Tinman* and *Seven up* GFP (Fig.4C). By knocking down *ND42* and *ND75* from the developing mesoderm using *Twist*Gal4 as a driver, a random increase in the number of *Seven up* positive cardioblasts is revealed (Fig.4D, G). Co-immunostaining with *Tinman* and *Seven up* revealed a corresponding reduction in *Tinman* positive cardioblasts (Fig. 4F, I) .These observations imply that a myogenic tentative *Tinman* expressing cardioblast has started expressing an ostial marker *Seven up*, and thus has changed its cell fate.

We tracked down this phenotype down the stages of heart tube formation and cell specifications. *Tinman* expression starts in the developing mesoderm from stage 9 (Zaffran et al., 2006). At stage 11, *Seven up* expression begins in a subset of cardiac progenitors. These progenitors are initially both *Tinman* and *Seven up* positive but at stage 12; they lose *Tinman* expression and retain *Seven up* only (Lo and Frasch, 2001).

In *ND42/ND75* knockdown embryos, *Seven up* expression is normal at stage 11. At stage 12 also, the total number of cells expressing *Seven up* is unchanged when compared to wild type embryos (Fig.S3). However at stage 13, when normal 4+2 pattern of *Tinman* + *Seven up* positive cells is present in control embryos, in *ND42/ND75* knockdown embryos, there were some *Tinman* positive cells that show a very low level of *Seven up* expression too, suggesting the onset of 2+4 instead of 4+2 pattern of cardioblasts initiated at stage 13 (Fig. 4J-R).

Quantitative analysis of region-specific fate specification defects in knockdown embryos:

Since the cell type alteration defect is very random in terms of change in different parts of the cardiac tube, we quantified this phenotype with respect to following criteria:

a) Number of embryos with defect in the aorta region only

b) Number of embryos with defect in heart proper region only

c) Number of embryos with defect in both the aorta and heart proper region

d) Number of embryos with no defect.

Out of the total 100 embryos analyzed for both *ND42* and *ND75* knockdown, the distribution of phenotype is shown with the pie chart (Fig.4.7S and T).

In case of *TwistGal4/+; UAS ND42dsRNA/+*, it was found that out of 100 embryos analyzed, 18 embryos show no cell fate alteration defect either in aorta or heart proper region. 32 embryos exhibit defects in aorta only whereas 20 embryo exhibit defects in heart proper region. 30 embryos exhibit severe defects i.e. in these embryos, cell fate specification defects were observed in aorta as well as heart proper regions (Fig.4S). In case of *TwistGal4/+; UAS ND75dsRNA/+*, it was found that out of 100 embryos analyzed, 22 embryos show no cell fate alteration defect either in aorta or heart proper region. 31 embryos exhibit defects in aorta only whereas 15 embryo exhibit defects in heart proper region. 32 embryos exhibit severe defects i.e. in these embryos, cell fate specification defects were observed in aorta as well as heart proper regions (Fig.4T).

Knockdown of genes encoding complex-I components leads to high ROS levels in the developing mesoderm

Elevated ROS levels were observed in *TwistGal4/+; UAS ND42RNAi/+* and *TwistGal4/+;UAS ND75RNAi/+* background using mitoSOX dye which specifically detects mitochondrial generated superoxide ions (Dikalova et al., 2010, Itani et al., 2016, Zielonka et al., 2008). Staining with mitoSOX revealed that the majority of mesodermal cells are positive for mitoSOX in *TwistGal4/+; UAS ND42RNAi/+* (Fig.5B) *and TwistGal4/+;UAS ND75RNAi/+* (Fig.5C) knockdown embryos at stage 13 of embryonic development compared to control embryos (Fig 5A) confirming the mitochondrial origin of ROS.

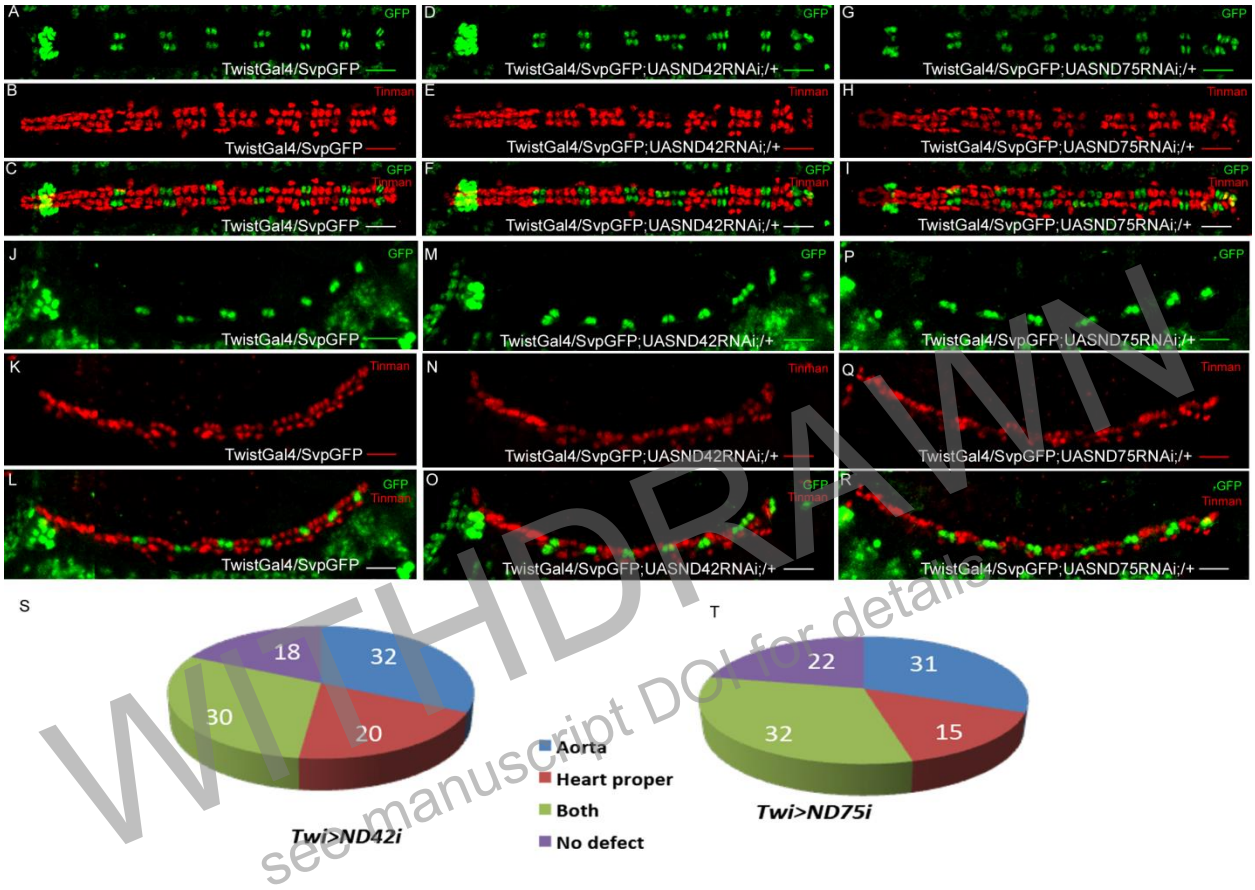

Fig.4 Cellular characterization of the cardiac tube revealed alteration in cell fate specification in complex-I knockdown embryos Wild type stage 16 *Drosophila* embryonic heart stained for *SevenupGFP* expressed in ring gland and two cardioblasts per hemisegment **(A).** *Tinman* is expressed in 4 cardioblasts per hemisegment in wild type stage 16 embryos **(B).** Co-immunostaining of *Tinman* and *Seven up* showed the 4+2 pattern of *Tinman+Seven up* cardioblasts in each hemisegment **(C).** In *ND42* and *ND75* knockdown embryos, there is an increase in *Seven up* positive cardioblasts in certain segments (**D, G).** Reduction in *Tinman* positive cardioblasts in some segments in *ND42* and *ND75* knockdown embryos **(E, H).** Co-immunostaining of *Tinman* and *Seven up* revealed an increase in *Seven up* positive cardioblasts correspond to reduced *Tinman* positive cardioblasts **(F, I).** There are some cardioblasts which co-express *Tinman* and *Seven up*. Alteration in cell fate specification initiates at stage 13 of embryonic development. Wild type stage 13 *Drosophila* embryo stained for *seven up* GFP, marking two cardioblasts per hemisegment **(J)** and *Tinman*, marking 4 cardioblasts per hemisegment **(K**) Co-immunostaining of Tinman and *Sevenup*GFP reveals 4+2 pattern of these two subpopulations **(L).** In *ND42* and *ND75* knockdown embryos, reduction in *tinman* positive cardioblasts **(N, Q)** is accompanied by an increase in number of *seven up* positive cardioblasts (**M, P)**There are some cells which are positive for both *tinman* and *seven up*, although expression of *tinman* is lowered compared to neighboring cells, suggesting fate change event has been initiated in these cells. (**O, R).** Quantization of cell fate defect with respect to its prevalence in aorta and heart proper regions of the cardiac tube at stage 16 of embryonic development **(S, T).** Scale bar: 20µm

Glutathione-S- transferase D1-GFP (*gstD* GFP) reporter construct has been previously shown to be *in vivo* sensor for ROS (Sykiotis and Bohmann, 2008). ROS activity was detected in the mesodermal population using *gst*D GFP construct in *TwistGal4/+; UAS ND42RNAi/+* (Fig.5E) *and TwistGal4/+;UAS ND75RNAi/+* (Fig.5F) knockdown embryos at stage 13 of embryonic development compared to control embryos (Fig 5D).

Co-localization of *Twist* expressing and high *gst* D GFP expressing mesodermal cells at stage 10 of embryonic development:

The elevated mitoSOX levels observed in the mesodermal derivatives of *TwistGal4/+;UAS ND42dsRNA/+(*Fig. 5B) and *TwistGal4/+;UAS ND75dsRNA/+* (Fig.5D)embryos were declined significantly by over expressing superoxide dismutase (*SOD2)* in the *ND42* and *ND75* knockdown embryos (Fig.5C,E). *GstD GFP* levels were significantly reduced to low levels in *TwistGal4/UAS SOD2;UAS ND42dsRNA/+* (Fig.5I) as well as *TwistGal4/UAS SOD2;UAS ND75dsRNA/+* knockdown embryos (Fig. 5K) compared to *TwistGal4/+;UAS ND42dsRNA/+(*Fig. 5H) and *TwistGal4/+;UAS ND75dsRNA/+* (Fig.5J) embryos. These results established that overexpression of *SOD2* is able to rescue elevated mitoSOX and *gst*D GFP levels.

Twist expression initiates at stage 10 of embryonic development in mesodermal progenitors and continues to express until stage 13 of embryonic development (Leptin, 1991). Since *Twist Gal4* is used to derive *UAS ND42RNAi* and *UAS ND75RNAi*, it can be expected that ROS levels are increased in *Twist* expressing mesodermal cells.

Co-immunostaining with *Twist* antibody and anti-GFP antibody in *TwistGal4gstD GFP/+; UAS ND42RNAi/+* and *TwistGal4gstD GFP/+; UAS ND75RNAi/+* embryos revealed that at stage 10 of embryonic development when *gst*D GFP expression initiates in the developing mesoderm, *Twist* expression overlaps exactly with *gst*D GFP expression in *ND42* and *ND75* knockdown embryos. This result shows that ROS levels are increased in *Twist* expressing mesodermal cells in *TwistGal4gstD GFP/+; UAS ND42RNAi/+* (Fig.5D, E and F) *and TwistGal4gstD GFP/+; UAS ND75RNAi/+* (Fig.5G,H and I) knockdown embryos at stage 10 of embryonic development compared to control embryos (Fig 5A,B and C).

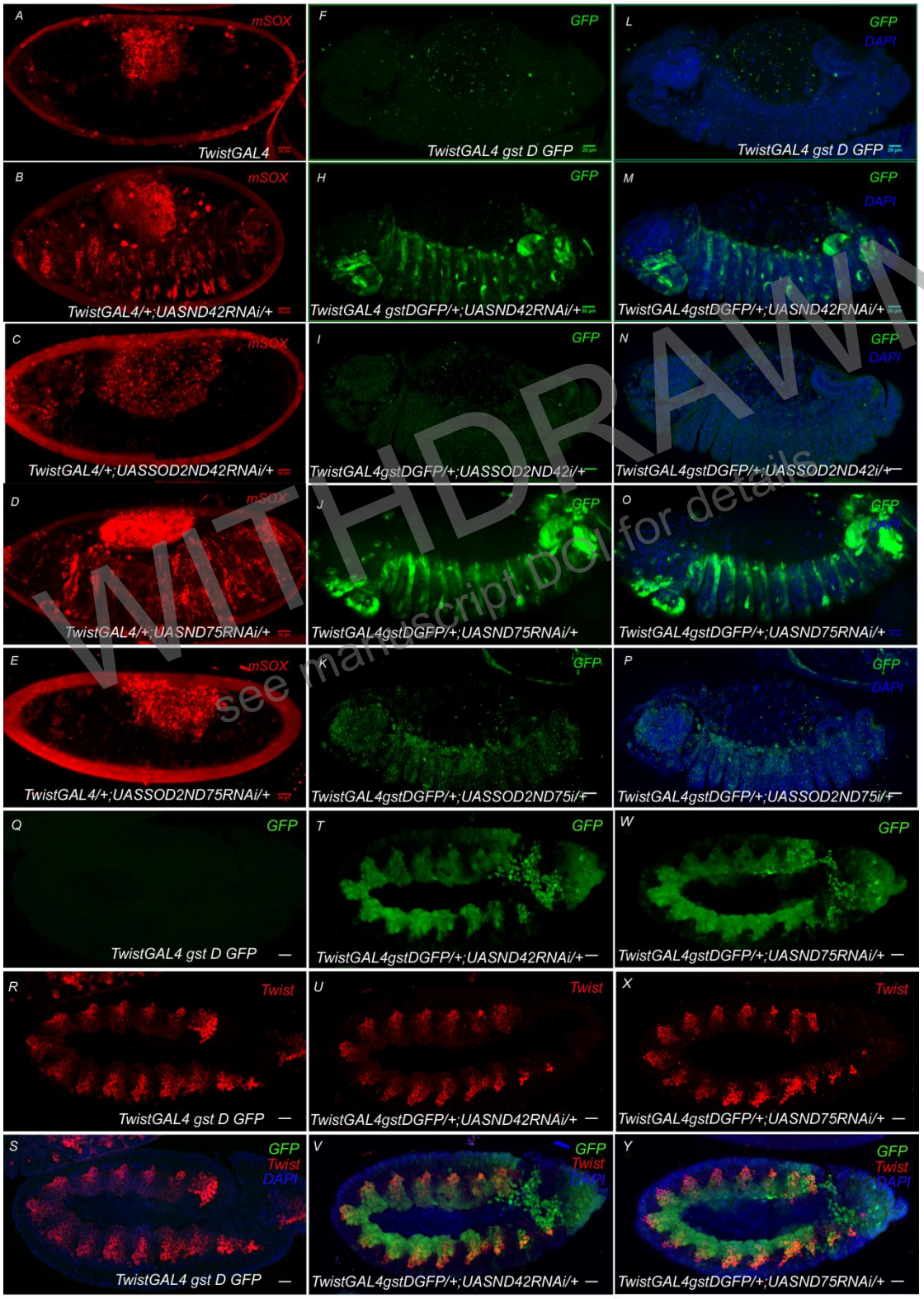

Fig.5. Knocking down genes encoding complex-I components from the developing mesoderm leads to high ROS levels in the mesodermal derivatives in the *Twist* expression specific manner : Wild type stage 13 embryo

stained for mitoSOX red **(A).** Mitosox staining can be located in each hemisegment in *ND42* and *ND75* knockdown embryos (**B, D**). Over-expression of *SOD2* in the *ND42* and *ND75* knockdown embryos is able to scavenge high ROS levels as suggested by visibly very low mitoSOX stain in these embryos (**C, E**). Wild type stage 13 embryos negative for *gstD* GFP expression (**F, L**). *ND42* and *ND75* knockdown embryos show a high level of *gst*DGFP expression in each hemisegment (**H, J**). Overexpression of SOD2 in these knockdown backgrounds leads to a significant reduction in *gst*D GFP levels in each hemisegment **(I, K).** Increase in ROS levels specifically in *Twist* expressing mesodermal cells. Wild type stage 10 *Drosophila* embryo stained negative for gstD GFP **(Q).** *Twist* expression in the mesodermal progenitors at stage 10 of embryonic development in wild type embryo **(R),** merged with DAPI (**S**). *ND42* knockdown embryo shows elevated *gst*D GFP expression in each hemisegment **(T**), co-immunostained with *Twist* antibody **(U).** Merged image shows co-local5ization of *gst*DGFP and *Twist* expression in the mesoderma cells (**V).** *ND75* knockdown embryo shows elevated *gst*D GFP expression in each hemisegment (**W)**, co-immunostained with *Twist* antibody **(X).** Merged image shows co-localization of *gst*DGFP and *Twist* expression in the mesoderma cells **(Y)** in knockdown embryos. Scale bar: 20µm

Over expression of *Superoxide dismutase 2* significantly restores the survival rate in *ND42* and *ND75* knockdown embryos:

Superoxide dismutase 2 (SOD2) specifically scavenges the superoxide ions generated during the mitochondrial electron transport chain (Fukai and Ushio-Fukai, 2011).

Lethality assay was done with total 1000 embryos in each case at 29 degrees to observe and quantify the hatching rate of embryos. It was found that in *TwistGal4/ UAS SOD2; UAS ND42 RNAi/+* genotype, around 54 % of embryos were hatched, a significant rescue in comparison to 20% embryos hatched in *TwistGal4/+;UAS ND42RNAi/+* progeny. A similar trend was observed in *TwistGal4/ UAS SOD2; UAS ND75 RNAi/+* background, where average 57% embryos were hatched compared to only 21% embryos hatched in *TwistGal/+; UAS ND75RNAi/+* progeny, thus showing a significant rescue (Fig. 6A) in hatching rate.

Scavenging ROS rescues the cardiac functionality to a significant level:

The alteration in the rhythmicity of the cardiac tube beating pattern observed in *TwistGal4/+;UAS ND42dsRNA/+* and *TwistGal4/+;UAS ND42dsRNAi/+* embryos is reportedly rescued by over-expressing *SOD2* in the respective backgrounds.

Cardiac tubes of stage 17 embryos from *HandGFP; TwistGal4/UAS SOD2; UAS ND42 RNAi/+* and *HandGFP; TwistGAL4 /UAS SOD2; UAS ND75 RNAi/+* genotypes were observed for beating patterns and the cardiac parameters were quantified using SOHA software.

Live imaging clearly indicate the restoration of regular beating pattern in the cardiac tube of *HandGFP; TwistGal4/UAS SOD2; UAS ND42 RNAi/+(*Movie 5) and *HandGFP; TwistGAL4 /UAS SOD2; UAS ND75 RNAi/+(*Movie 6) embryos.

M-mode patterns of *HandGFP; TwistGal4/UAS SOD2; UAS ND42 RNAi/+* (Fig.6C) and *HandGFP; TwistGAL4 /UAS SOD2; UAS ND75 RNAi/+* (Fig.6E) genotypes show a significant restoration to the periodic M-mode pattern.

Heart period of stage 17 knockdown embryos in *SOD2* overexpression background:

As reported previously, the heart period is increased to around 3 fold in *ND42* and *ND75* knockdown embryos compared to the control. Interestingly, by over-expressing *SOD2* in *ND42* and *ND75* knockdown embryos, the heart period is significantly reduced towards normal. In case of *HandGFP; TwistGal4/UAS SOD2; UAS ND42RNAi/+* embryos, the heart period is 8.98 milliseconds which is a significant reduction from the heart period of 15.15 milliseconds in *HandGFP;TwistGal4/+; UAS ND42RNAi/+* embryos.

In case of *HandGFP; TwistGal4/UAS SOD2; UAS ND75RNAi/+* embryos, the heart period is 8.06 milliseconds which is a significant reduction from the heart period of 14.64 milliseconds in *HandGFP; TwistGal4/+; UAS ND75RNAi/+* embryos (Fig.6J).

Diastolic interval is reduced in the knockdown embryos by over-expression of *SOD2*:

By scavenging superoxide ions specifically from the mesoderm population, DI is reduced significantly in *ND42* (1.10 ms) and *ND75* knockdown embryos (0.95 ms) compared to *HandGFP;TwistGal4> UAS ND42dsRNA* (2.92ms) and *HandGFP;TwistGal4> UAS ND75dsRNA* embryos (2.63ms) (Fig.6H).

Systolic interval is increased in knockdown embryos by over-expression of *SOD2* in *Twist* expressing mesoderm population:

Systolic interval was reportedly reduced drastically in *HandGFP; TwistGAL4 /+; UAS ND42RNAi/+*(SI=0.15ms) and *HandGFP; TwistGal4 /+; UAS ND75RNAi/+* (SI=0.15ms) knockdown embryos compared to control (SI=0.52ms). It was found that SI is significantly increased in *HandGFP; TwistGAL4 /UAS SOD2; UAS ND42 RNAi/+* (SI=0.67ms) and *HandGFP; TwistGAL4 /UAS SOD2; UAS ND75 RNAi/+* knockdown embryos (SI=0.6m1s) (Fig.6I).

Systolic and diastolic diameters are restored to normal by scavenging superoxide ions:

Systole diameter (SD) and diastole diameter (DD) in *HandGFP; TwistGAL4 /UAS SOD2; UAS ND42 RNAi/+* (SD=61.87 microns, DD =96.83 microns) and *HandGFP; TwistGAL4 /UAS SOD2; UAS ND75 RNAi/+* embryos (SD= 64.57 microns, DD= 95.52 microns) are significantly increased compared to *HandGFP; TwistGAL4 /+; UAS ND42 RNAi/+* (SD=27.77 microns, DD =43.73 microns) and *HandGFP; TwistGAL4/+; UAS ND75 RNAi/+* embryos (SD= 32.65 microns, DD= 45.19 microns) (Fig. 6F, G).

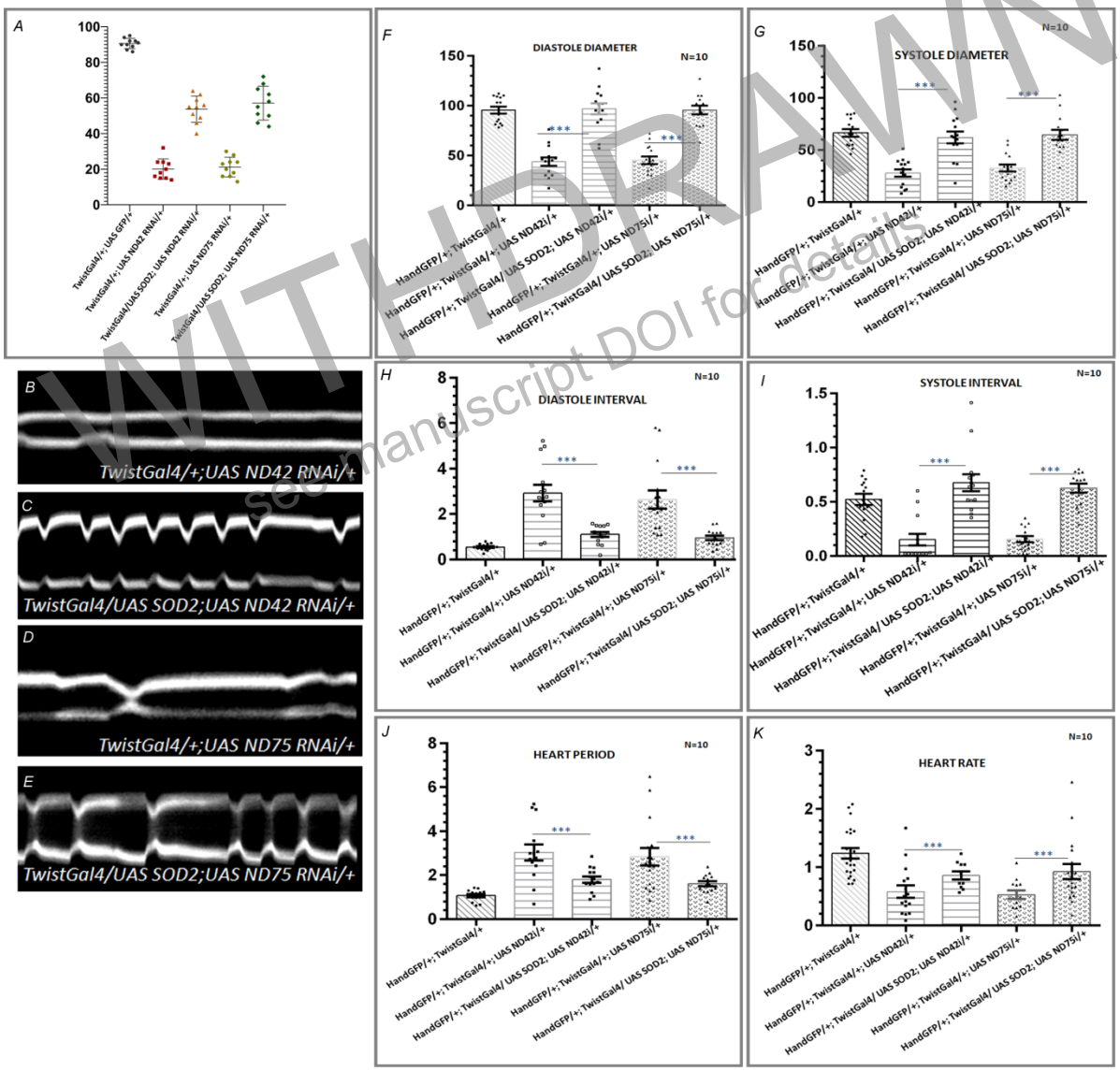

Fig. 6. Scavenging superoxide ions rescues embryonic lethality and restores functionality of the cardiac tube: Statistical analysis of hatching rate of embryos revealed significant rescue in *TwistGal4/UAS SOD2; UAS ND42 RNAi/+* and *TwistGal4/UAS SOD2; UAS ND75 RNAi/+* embryos compared to *TwistGal4/+; UAS ND42 RNAi/+*

and *TwistGal4/+; UAS ND75 RNAi/+* knockdown embryos (n=1000) **(A)** .M-mode of *TwistGal4/UAS SOD2; UAS ND42 RNAi/+(***C)** *and TwistGal4/UAS SOD2; UAS ND75 RNAi/+ (***E)** shows more periodic movements of heart wall with time as compared to M-mode in *TwistGal4/+; UAS ND42 RNAi/+(***B)** and *TwistGal4/+; UAS ND75 RNAi/+(***D)** knockdown embryos**.** Quantization of cardiac parameters with SOHA revealed significant rescue in heart rate, heart period, systole-diastole interval and systole-diastole diameters by scavenging superoxide ions from the developing mesoderm **(F-K)**

High ROS levels are responsible for complex I attenuation induced lumen constriction and *Pericardin* over expression in the dorsal vessel

The lumen diameter was measured in *TrolGFP; TwistGal4/UAS SOD2; UAS ND42 RNAi/+* and *TrolGFP; TwistGal4/UAS SOD2; UAS ND75 RNAi/+* embryos. Lumen diameter was significantly restored in *TrolGFP, TwistGal4/UAS SOD2; UAS ND42 RNAi/+* and *TrolGFP, TwistGal4/UAS SOD2; UAS ND75 RNAi/+* embryos compared to their knockdown counterparts. In case of *TrolGFP, TwistGal4/UAS SOD2; UAS ND42 RNAi/+* embryos, lumen diameter was increased from 1.5 um in *TrolGFP, TwistGal4/+; UAS ND42 RNAi/+* (Fig.7C) to 2.22 um in aorta region in *TrolGFP, TwistGal4/UAS SOD2; UAS ND42 RNAi/+* embryos. (Fig.7E). The lumen diameter in heart proper region was increased from 1.95 microns in *TrolGFP, TwistGal4/+; UAS ND42 RNAi/+*to 2.69um in *TrolGFP, TwistGal4/UAS SOD2; UAS ND42 RNAi/+* (Fig.7F) embryos (Fig.7D). A similar trend was observed in *TrolGFP, TwistGal4/UAS SOD2; UAS ND75 RNAi/+* where lumen diameter was increased from 1.55 um (Fig.7G) to 2.07 um (Fig.7I) in aorta and 2.42um (Fig.7J) from 1.93 um in heart proper (Fig.7H).

Transcriptional upregulation of *Pericardin* is rescued by scavenging superoxide ions:

High *Pericardin* levels observed in *TwistGal4/+; UAS ND42RNAi/+*and *TwistGal4/+; UAS ND75RNAi/+* embryos (Fig.7N and P) were decreased in *TwistGal4/UAS SOD2; UAS ND42RNAi/+* and *TwistGal4/UAS SOD2; UAS ND75RNAi/+* embryos (Fig. 7O and Q) as revealed by *Pericardin* immunostaining. *Pericardin* was much more restricted outside the lumen of the cardiac tube and *Pericardin* expression resembles closer to control embryos.

qRT PCR of *TwistGal4/UAS SOD2; UAS ND42RNAi/+* knockdown embryos revealed that *Pericardin* transcript levels were reduced significantly compared to knockdown embryos (Fig.7R) .A similar trend was shown by *TwistGal4/UAS SOD2; UAS ND75RNAi/+* embryos

where *Pericardin* transcript levels were reduced compared to high levels in *ND75* knockdown embryos (Fig.7S).

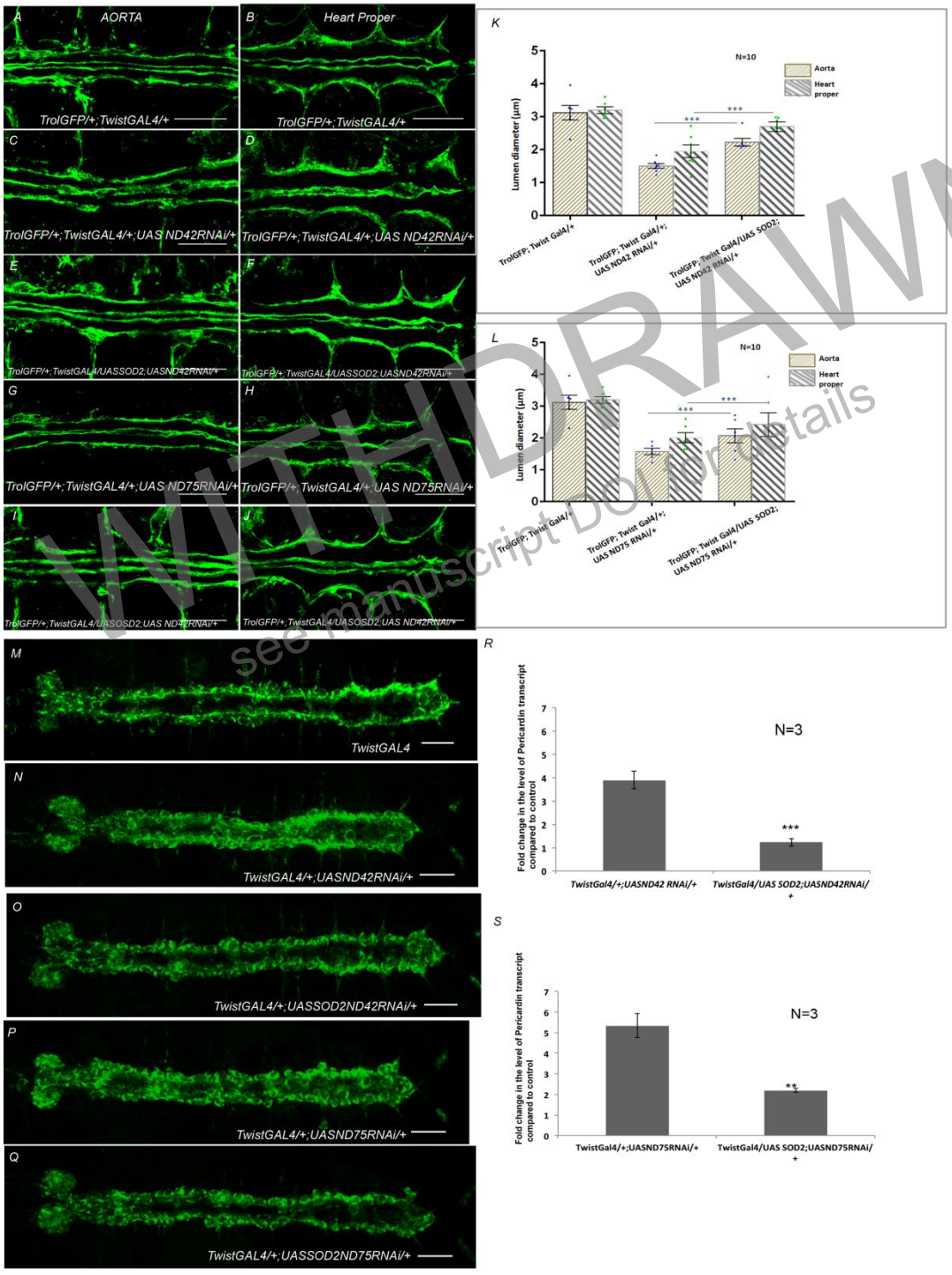

Fig. 7. Significant restoration of luminal diameter by scavenging superoxide ions from developing mesoderm: *TrolGFP* expression in the Aorta region **(A)** and Heart Proper (**B)** of wild type stage 16 *Drosophila* embryonic heart. Knockdown of *ND42* and *ND75* from the developing mesoderm leads to constriction of lumen in aorta as well as

heart proper regions (**C, D, G, H**). Lumen diameter is evidently restored in *TwistGal4/ UAS SOD2; UAS ND42 RNAi/+* and *TwistGal4/ UAS SOD2; UAS ND75 RNAi/+* embryos in the aorta **(E, I**) as well as heart proper region. **(F, J)** Statistical analysis revealed a significant rescue in lumen diameter in *SOD2* backgrounds compared to their knockdown counterparts **(K, L).** Increased *Pericardin* expression in the cardiac tube of *ND42* and *ND75* knockdown embryos is rescued by overexpressing *SOD2*: Wild type stage 16 *Drosophila* embryonic heart immunostained for *Pericardin*, whose expression is confined at the boundaries of cardiac tube **(M).** Knockdown of *ND42* and *ND75* leads to increased and mislocalized *pericardin* expression **(N, P).** Overexpression of *SOD2* in the ND42 and ND75 knockdown embryos leads to the reduction and restriction of *Pericardin* expression around the cardiac tube boundaries **(O, Q).** *Pericardin* transcript levels are significantly restored to normal in *TwistGal4/ UAS SOD2; UAS ND42 RNAi/+* and *TwistGal4/ UAS SOD2; UAS ND75 RNAi/+* embryos as revealed by qRT PCR **(R, S).** Scale bar: 20µm

High level of ROS in the developing cardiogenic mesoderm is responsible for alteration in cell fate specification:

In order to investigate whether increased ROS levels in the cardiogenic mesoderm was responsible for alteration in cell fate specification which initiate from stage 13 of embryonic development, *Tinman* vs *Seven up* subpopulations were observed in *TwistGal4/UAS SOD2; UAS ND42RNAi/+ and TwistGal4/UAS SOD2; UAS ND75RNAi* embryos.

As described previously, knocking down *ND42* from the developing mesoderm result in increase in number of *Seven up* positive cardioblasts (Fig. 8D) in the cardiac tube of stage 16 *Drosophila* embryo compared to control (Fig. 8A). In these embryos, there is a simultaneous reduction in number of *Tinman* positive cardioblasts (Fig. 8E).By scavenging ROS by over expressing *super-oxide dismutase 2 (SOD2)* in these knockdown embryos lead to restoration of normal 4+2 pattern of *Tinman vs Seven up* cardioblasts as shown by co-immunostaining for *Tinman* and *Seven up* (Fig.8 G, H and I).

Knocking down *ND75* from the developing mesoderm also result in increase in number of *Seven up* positive cardioblasts (Fig. 8J) in the cardiac tube of stage 16 *Drosophila* embryo compared to control(Fig.8A). In these embryos, there is a simultaneous reduction in number of *Tinman* positive cardioblasts (Fig. 8K). Scavenging ROS by over expressing *superoxide dismutase 2* (*SOD2*) in these knockdown embryos lead to restoration of normal 4+2 pattern of *Tinman vs Seven up* cardioblasts as shown by co-immunostaining for *Tinman* and *Seven up* (Fig.8 M, N and O). Quantitative analysis of region specific defects in aorta, heart proper region and both of these regions showed that over expression of *SOD2* in knockdown embryos led to significant

restoration towards normal 4+2 pattern of *Tinman* vs *Seven up* cardioblasts in these embryos (Fig.8P and Q).

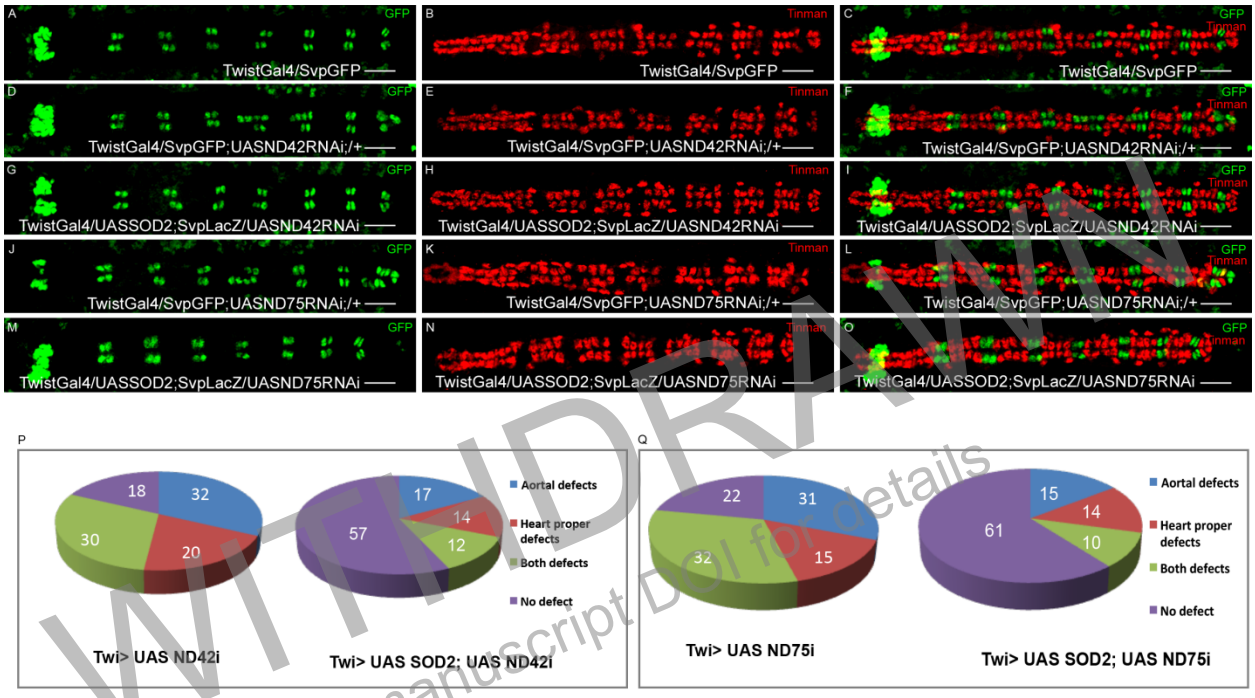

Fig.8. Scavenging ROS from the developing mesoderm is able to reverse cell fate specification defects in complex-I knockdown embryos. *Seven up*(**A),** *Tinman* **(B**) and co-expression of *Tinman* and *Seven up* (**C)** in wild type stage 16 *Drosophila* embryonic heart. In *ND42* and *ND75* knockdown embryos, reduction in *Tinman* positive cardioblasts is complemente d by an increase in *seven up* positive cardioblasts (**F, L).** Overexpression of *SOD2* in *ND42* and *ND75* knockdown backgrounds lead to the significant restoration of the normal 4+2 pattern of *Tinman+ seven up* cardioblasts. **(I, O**). Quantitative analysis of region-specific defects shows significant rescue in the number of defective embryos in *SOD2* overexpression background (**P, Q).**

MATERIALS AND METHODS

Fly stocks:

The fly stocks used were *Twist*Gal4 (BL2517, *Mef2*Gal4 (BL27390), *Tinc delta4* Gal4 (M. Frasch), *Hand*Gal4 (E. Olson), *Da*Gal4 (BL8641), UAS *nlsGFP* (BL6294), UAS *SOD2* (BL24494), *ND42*(G4500) (BL30085), *gstD-GFP* (gifted by D. Bohmen), *HandGFP*; *Sco/cyo* (gifted by E. Olson), *Zcl1700* (L. Cooley) , *SvpGFP* (R. Spokony), UAS *ND42* RNAi (BL32998), UAS *ND75* RNAi (BL33910).

All stocks and crosses were maintained at 25° C, except for those used in RNAi and Gal4/UAS expression experiments. In those cases, crosses were kept at 29°C.

For embryo collection, flies are acclimatized to the plate conditions by transferring them to food plates overnight at 25°C (for *RNAi* experiments, flies were reared at 29°C). The next day, synchronized egg collections are set on fruit plates and enriched for desired stages.

Embryo fixation:

Embryos from the synchronized collection were transferred from plate to a mesh using a small paintbrush by squirting distilled water over the plate. A quick wash of distilled water was given to the embryos to remove unwanted debris and yeast paste. After that, embryos were dechorionated by treating them with 50 percent sodium hypochlorite solution (bleach) for 2 minutes. Bleach was removed by thoroughly washing embryos with distilled water for 3*10' (3 washes, 10 minutes each).

In the meantime, a fixative (PEMS+4% formaldehyde + heptane) was prepared in the ratio of 7:1:7 in the scintillation vial. Embryos were incubated in the fixative for 40 minutes on a nutator. After fixation is over, the lowermost layer of fixative solution which is comprised of heptanes is removed and replaced by an equal volume of methanol. The resulting two membrane solution is shaken vigorously to facilitate removal of the vitelline membrane. The devitellinized embryos are settled down and are collected with the help of a dropper in a fresh Eppendorf tube. Again, the lowermost layer is removed and methanol of equal volume of the leftover solution is added further and the same process is repeated until all devitellinized embryos are harvested.

After collecting embryos in the eppendorf tube, methanol is replaced by absolute ethanol and after a quick wash of 5 minutes with ethanol; these embryos are either used for immunostaining or are stored in absolute ethanol at -20°C for future use.

Live Imaging of *Drosophila* Embryos:

All collections were kept at 29 degrees since Gal4 induced RNAi knockdown efficiency is maximum at this temperature. Synchronized egg laying was set for stage 17 embryo collection. Embryos were harvested as mentioned earlier in a mesh and dechorionated using sodium

hypochlorite solution. After treating with bleach, embryos were thoroughly washed with distilled water (4 washes of 10 minutes each) to completely remove bleach as it can interfere with the fluorescence signal.

After washings, distilled water was replaced with 1X PBS in the mesh containing embryos. With the help of a fine paintbrush, the embryos of stage 17 were transferred from mesh to halocarbon oil placed on the glass slide. A bridge was made using nail paint on both sides of the halocarbon oil drop containing embryos and after nail paint is dried, a coverslip is placed on the bridge on such a level that embryo is only stabilized and not mashed with the coverslip.

Live imaging was performed in the fluorescence microscope (model name and number) using FITC filter at 20x magnification and analyzed using SOHA (Semi-automated Heart Beat Analysis) software.

Semi-Automated Heartbeat analysis of *Drosophila* embryos:

SOHA (Semi-automated heartbeat analysis) software was used to analyze a number of contraction-relaxation parameters in *Drosophila* embryonic heart. SOHA incorporates a unique set of movement detection algorithms that automatically and precisely detect and measure beat to beat contraction parameters captured in live movies, therefore providing both analytical and statistical power. The resulting output provides detailed information related to pacemaker activity and contraction-relaxation parameters including M-mode, heart rate, systolic interval and diastolic intervals, systolic and diastolic diameters and fractional shortening (Ocorr et al., 2009).

Before analyzing these parameters in knockdown embryos relative to control, these different parameters are briefly defined as follows:

1. M-mode: represents the vertical movement of heart tube edges (y-axis) over time (x-axis)
2. Heart period: is measured as the interval between the start of one diastole and the beginning of the next.
3. Systolic interval (SI): SI is the duration for which cardiac tube stays in the systolic (contraction) phase.

4. Diastolic interval: (DI): is the duration for which the heart stays in the diastolic (relaxation) phase.
5. Systolic diameter: represents the contracted state of the heart tube.
6. Diastolic diameter: represents the relaxed state of the heart tube.

Immunohistochemistry and Imaging:

Embryos stored in ethanol at -20 degrees are brought to room temperature by keeping at room temperature (RT) for 15 minutes. After replacing ethanol by 0.1%PBT, embryos were given 3 subsequent washes with 0.1% PBT, 10 minutes each at nutator, RT. Washes are followed by 1 hour incubation of embryos in blocking solution (10X NGS in 0.1%PBT) for 1 hour at nutator, RT. Primary antibody made in 10X NGS in 0.1%PBT is added, embryos were incubated in primary antibody overnight at 4 degrees kept on nutator. The secondary antibody is prepared in 10X NGS and embryos are incubated in the secondary antibody overnight at a nutator, 4 degrees C. From this step onwards, the vial containing embryos is to be covered with aluminum foil to prevent photobleaching of secondary antibody. After replacing secondary antibody with 0.1% PBT, subsequent 3 washes with PBT of 10 minutes each are given at nutator, RT.After the staining, PBT is replaced by DAPI Vectashield and embryos are mounted in DAPI Vectashield to observe under fluorescence or confocal microscope.

Immunofluorescence images were captured in the Laser Scanning Confocal Microscope (LSM 780, Carl Zeiss). Optical sectioning was done using line mode in the confocal microscope. Images were analyzed and processed using the software ImageJ.

Primary antibodies used were Mef2 (1:1000, gifted by H.Nguyen), anti b-galactosidase (1:100, Promega Z3781), antiGFP (1:100, Sigma G6539), Pericardin (1:3, DSHB EC11), Twist (1:1000, gifted by Maria Leptin), Seven up (1:500), Tinman (1:1000, gifted by Manfred Frasch), Zfh1 (1:1000), Even skipped (1:10, DSHB 3C10), Odd (1:1000, gifted by Skeath), Antennapedia (1:5, DSHB, 4C3). The secondary antibodies used were FITC conjugated anti-mouse (Jacksons Immuno Research Laboratories, 115–095-166), polyclonal Cy3 conjugated anti rabbit (Jacksons Immuno Research Laboratories, 711–165-152), polyclonal Cy3 conjugated Anti-mouse (Jacksons Immuno Research Laboratories, #115-165-166), and FITC conjugated anti rabbit (Jacksons Immuno Research Laboratories, #711-165-153) at 1:400 dilution.

Statistical analysis of lumen diameter of cardiac tube in stage 16 *Drosophila* embryos:

In order to measure lumen diameter of cardiac tube marked by *Trol*GFP, cardiac tube was subdivided into anterior aorta and posterior heart proper region. In both of these parts of the cardiac tube, 5 points of measurements were taken from each segment. Average of these measurements was calculated to infer readings for each sample.

MitoSOX dye labeling of *Drosophila* embryos:

Embryos were transferred from the fruit plate to the sieve with the help of a paint brush. Embryos were treated with bleach for 2 minutes to remove chorion. After that, they were given 4 washes of 10 minutes each with distilled water for complete removal of bleach. Embryos were dehydrated with 100% isopropanol for 40 seconds followed by pat drying to remove isopropanol. After that, embryos were treated with hexane for 4 minutes followed by pat drying to remove hexane. Embryos were washed using 1X Ringer's solution containing 0.1%BSA for 2 minutes on a shaker. Sieve containing embryos was soaked in msox solution (1:5000 in 1X PBS). Volume was kept to a level that all embryos get immersed in the dye solution. They were incubated in the dye for 25 minutes. Embryos were washed off with Ringer's solution for 2 minutes on a shaker. Embryos were mounted in halocarbon oil and imaged under the confocal microscope.

ATP Assay:

ATP assay was performed from control, ND42 and ND75 knockdown embryos of stage 16 embryonic development. Embryos were suspended in 1X PBS (ph=7.2) and homogenized in ATP assay Lysis buffer (6 M Guanidine-HCl, 100 mM Tris pH 8 and 4 mM EDTA, all from Sigma Aldrich, Cat# G3272, Cat# T5941 and Cat# EDS-100G respectively) (Tsai et al., 2014). The samples were boiled at 95^0C for 5 minutes and diluted 1:1000 in dilution buffer provided in ATP luminescence kit HSII (Roche, Cat# 11699709001). The further assay was performed as instructed by the kit's manual in Luminometer (Promega GloMax96 Microplate Luminometer). A standard curve was generated and ATP concentrations were calculated. The ATP concentration was normalized with protein concentration as determined by Bradford method (the details are provided later in the protein extraction method).

Mitochondria Isolation:

Mitochondria isolation was performed by Mitochondrial Isolation Kit (Sigma Aldrich, Cat# MITOISO1-1KT) according to the manual's instruction. Larvae were washed and homogenized in 1X Extraction Buffer A with 0.1 mg/ml. Homogenate was centrifuged at 600 X *g* for 5 minutes at 4^0C. The supernatant was centrifuged at 11,000 X *g* for 10 minutes. The pellet was resuspended in 1X Extraction Buffer A and recentrifuged as above. The pellet was resuspended in 1X Storage Buffer and stored at -20^0C.

Complex I Assay:

The isolated mitochondria samples were thawed at room temperature. 3 µl of purified mitochondrial were 150µl of prepared colorimetric complex I activity assay buffer (1X PBS, 3.5 g/l BSA, 0.2 mM NADH (Cat# N4505, 0.24 mM KCN: Cat# 1.04967, 60 mM DCIP: Cat# 33125, 70 mM decylubiquinone: Cat# D7911, 25 mM Antimycin A: Cat# A8674; all from Sigma Aldrich). NADH: ubiquinone oxidoreductase activity as a drop in DCIP absorbance was recorded at 600 nm on POLARstar Omega (BMG-LABTECH) for 180 seconds at an interval of 30 seconds. Rotenone insensitive activity was measured as the difference in DCIP reduction in the presence of 2 mM rotenone (Sigma Aldrich, Cat# R8875) in the assay buffer.

Citrate synthase Assay:

Mitochondrial samples were diluted to 10 fold in storage buffer. 5 µl diluted mitochondria sample was added to 150 µl of a previously prepared colorimetric citrate synthase activity assay buffer (50 mM Tris (pH 8.0), 0.1 mM 5, 5'-dithiobis- (2-nitrobenzoic acid) (DTNB Cat# D8120, 0.3 mM acetyl-CoA: Cat# A2056, 1 mM oxaloacetic acid : Cat# D4126). Citrate synthase activity was measured as an increase in DTNB absorbance at 412 nm using the POLARstar Omega (BMG-LABTECH) for180 seconds at the interval of 30 seconds. Finally, to determine the actual Complex I activity, the Rotenone sensitive NADH: ubiquinoneoxidoreductase activity was normalized with citrate synthase activity (Cho et al., 2012).

RNA isolation from embryos on Column

An appropriate number of (200 embryos) synchronized embryos were collected and dechorionated using sodium hypochlorite (bleach). Embryos were thoroughly washed with distilled water to remove bleach. Dechorionated embryos were homogenized in Trizol (Ambion,

Cat# 15596018) and extracted with 200µl of chloroform (Sigma Aldrich,Cat# C2432). Further purification was performed by using the RNeasy Mini Kit (Qiagen) as instructed. 25 minutes incubation at 37^0c was given with RNase free 2U DNase (Qiagen-79254) in RDD buffer to remove residual DNA. The RNA pellet was dissolved in nuclease-free DEPC treated water (Sigma).Quantitation of RNA was performed by using nanodrop spectrophotometer (GenovaNano, JENWAY). The quality of the isolated RNA was also verified by determining the ratio of the absorbance at 260nm/280nm and 260/230nm.

cDNA Synthesis and RT-qPCR

cDNA was synthesized using Verso cDNA synthesis kit (Thermo Scientific, Cat# AB1453A) following the manufacturer's recommended protocol. 500 ng of the template RNA was mixed with cDNA reaction mix (Verso Reverse Transcriptase, cDNA synthesis buffer, anchored OligodT primers, random hexamers and RT enhancer that degrades any ds DNA during the transcription of RNA) and incubated at 42ºC for 30 minutes and then kept at 95ºC for 2 minutes. Real time-qPCR (RT-qPCR) was conducted using the Bio-Rad CFX96 Touch Real-Time PCR Detection System. iTaqTM Universal SYBR Green Supermix from Bio-Rad (Cat# 172-5124) was used for the RT-qPCR reactions. To determine the optimal Tm for each primer set, graded RT-qPCR was performed. Fold inductions in transcript level were determined using the DDCt method. The transcript levels were normalized to either actin or tubulin transcript levels. RT-qPCR experiments were conducted on 3 to 4 independent cDNA samples per condition. The figures represent the combined data from all samples. Primers were so designed that they span the exon-exon junction. A list of primers used in our RT-qPCR experiments is available in Table S1.

Quantification and statistical analysis

In general, the quantitative analysis of data was performed and graphs were plotted in MS-Excel. Unpaired Student's T-Test was employed to determine statistical analysis, and N number as specified in graphs. The result of T-Test analysis is expressed in graphs in form of asterix as follows *p<0.05; **p<0.01 and ***p<0.001.

Discussion

Cardiac functionality is severely affected by knocking down genes encoding complex-I components of ETC from the mesoderm. These results indicate the importance of mitochondrial health for the cardiac tube to initiate its first beat and suggest the critical role metabolic dysfunction can play in congenital heart diseases.

The lethality associated with complex-I knockdown in embryos was shown to be specific to *ND42* and *ND75* knockdown as no lethality was observed with knockdown of GFP from the developing mesoderm using *Twist Gal4* driver. Since the average number of embryos that exhibit embryonic lethality was in concordance with an average number of embryos exhibiting cardiac malfunctioning, it was inferred that embryonic lethality was due to cardiac malfunctioning during embryonic development.

It was surprising to observe that despite the severe effect on cardiac functionality in knockdown embryos, we did don't see any gross change in the total number and alignment of cardioblasts as inferred by *Mef2* immunostaining (Fig.S2). No gross change in the total number of cardioblasts suggests that complex-I attenuation does not cause any cell death during cardiogenesis neither is there any abrupt increase in the total number of cardioblasts as previously shown for Notch mutant embryos (Grigorian et al., 2011). However, we see a drastic increase in *Pericardin* which is an ECM component. These results suggest that metabolic dysfunction imparts very specific effects with respect to genes that are affected. It is quite possible that *Pericardin* transcription is sensitive to the metabolic status of the pericardial cells, which is why the altered metabolic status of the cell induced high *Pericardin* expression. Not much is known about the regulation of *Pericardin* expression in embryos. However, in larval stages of *Drosophila* life cycle, *Pericardin* secretion has been shown to be affected by adipocyte-specific knock-down of Sar1 expression thus affecting the formation of a proper heart ECM in Drosophila. In adult *Drosophila* heart, high sugar diet conditions have shown to cause deterioration of heart function accompanied by increased *Pericardin* accumulation thereby creating fibrosis-like conditions (Na et al., 2013).

A collagen network is very important for the heart because it provides tensile strength as well as elasticity to allow the heart to operate normally in terms of systolic and diastolic functions (Weber et al., 1994). Collagen turnover is of utmost importance to maintain the balance between degradation and synthesis of collagen and imbalance of this turn over leads to excess collagen accumulation which ultimately leads to cardiac fibrosis (Iwanaga et al., 2002, Baicu et al., 2003,

Wang et al., 2006, Beltrami et al., 1994, Khan and Sheppard, 2006). Renin-angiotensin-aldosterone system (RAAS) has been shown to regulate this dynamic collagen turn over and intervention of this system can prevent the process of fibrosis (Weber and Brilla, 1991).Redox fibrosis, the term given to fibrosis that is caused by a high ROS level in the system is a hot area of research. Oxidative stress has been shown to be increased in various cardiac pathologies including hypertension, cardiac fibrosis, and heart failure (Robinson et al., 2012, Aragno et al., 2008, Cucoranu et al., 2005, Murdoch et al., 2006). An increase in ROS levels has been shown to play a critical role in the development and progression of cardiac remodeling associated with heart failure (Purnomo et al., 2013).The defects in mitochondrial OXPHOS has been reported to be one of the leading cause for prenatal and neonatal cardiomyopathies (Loeffen et al., 2001, Loeffen et al., 2000). A fetus diagnosed with hypertrophic cardiomyopathy at 37 weeks of gestation was found to have mitochondrial OXPHOS defect. These cardiomyopathies are more often hypertrophic than dilated (Garcia-Diaz et al., 2013). However, there are still a lot of unexplored aspects in this area specifically in the direction of pinpointing how altered metabolic dysfunction can lead to change in expression levels of ECM components. Our study has shed light on possibilities of ROS involvement in regulating levels and patterns of *Pericardin* expression specifically in complex-I deficit cardiogenic mesoderm. Hence, it can be a wonderful system to understand how metabolic perturbations can cause the alteration in ECM to induce cardiomyopathies.

The result that high ROS levels can directly alter the choice of fate a cell adopts is a groundbreaking finding. It has improved our understanding of the impact of retrograde signaling by mitochondria to regulate nuclear gene expression. There is a significant amount of research claiming the signaling pathways regulated by ROS (Zhang et al., 2013, Sena and Chandel, 2012, Giorgio et al., 2007, Liochev, 2013, Rhee, 2006, Wojtovich et al., 2019, Matsuzawa and Ichijo, 2005); however, the question whether metabolic status of a cell can determine the cell fate is still least explored.

Tinman and *seven up* positive cells are two different kinds of cardioblast populations with very different functions. *Tinman* positive cardioblasts are myocardioblasts which function as heart muscles and facilitate heart pumping (Bodmer, 1993). On the other hand, *seven up* positive cardioblasts are non-muscle cells that act as inflow tracts for hemolymph (Lo and Frasch, 2001).

Our finding implies that by sensing oxidative stress, a cascade of events started in the cardioblast to force it to adopt a completely different fate. This finding adds a new aspect to the regulation of cardiogenesis. Apart from the key signaling pathway s known to regulate cell fate specifications during cardiogenesis, reactive oxygen species have emerged out to be a key signal that has the capability to change course of events leading to altered cell fate of cardioblasts.

Implication of mitochondrial signaling in cell lineage specification and cardiogenesis has been shown by relatively fewer reports. Hom et al, 2011 has demonstrated that modulators of Mptp closure (mitochondrial permeability transition pores) promote mitochondrial maturation and cardiomyocyte differentiation in the mouse embryo (Folmes et al., 2012). In sea urchin embryos, oral-aboral axis specification has been shown to be entrained by mitochondrial distribution and redox state (Coffman and Davidson, 2001). The present study has added a new aspect to this field by showing that mitochondrial perturbations can directly hit the developmental programs and can reinforce the nuclear decisions to change the cell fate. Deciphering mechanisms underlying mitochondrial signaling in heart development may refine research on stem cell specification for regenerative applications thereby offer implications for cardiac pathology.

ARAGNO, M., MASTROCOLA, R., ALLOATTI, G., VERCELLINATTO, I., BARDINI, P., GEUNA, S., CATALANO, M. G., DANNI, O. & BOCCUZZI, G. 2008. Oxidative stress triggers cardiac fibrosis in the heart of diabetic rats. *Endocrinology,* 149**,** 380-8.

BAICU, C. F., STROUD, J. D., LIVESAY, V. A., HAPKE, E., HOLDER, J., SPINALE, F. G. & ZILE, M. R. 2003. Changes in extracellular collagen matrix alter myocardial systolic performance. *Am J Physiol Heart Circ Physiol,* 284**,** H122-32.

BELTRAMI, C. A., FINATO, N., ROCCO, M., FERUGLIO, G. A., PURICELLI, C., CIGOLA, E., QUAINI, F., SONNENBLICK, E. H., OLIVETTI, G. & ANVERSA, P. 1994. Structural basis of end-stage failure in ischemic cardiomyopathy in humans. *Circulation,* 89**,** 151-63.

BENHAOURECH, S., DRIGHIL, A. & HAMMIRI, A. E. 2016. Congenital heart disease and Down syndrome: various aspects of a confirmed association. *Cardiovasc J Afr,* 27**,** 287-290.

BENIT, P., BEUGNOT, R., CHRETIEN, D., GIURGEA, I., DE LONLAY-DEBENEY, P., ISSARTEL, J. P., CORRAL-DEBRINSKI, M., KERSCHER, S., RUSTIN, P., ROTIG, A. & MUNNICH, A. 2003. Mutant NDUFV2 subunit of mitochondrial complex I causes early onset hypertrophic cardiomyopathy and encephalopathy. *Hum Mutat,* 21**,** 582-6.

BODMER, R. 1993. The gene tinman is required for specification of the heart and visceral muscles in Drosophila. *Development,* 118**,** 719-29.

BRANDALIZE, A. P., BANDINELLI, E., DOS SANTOS, P. A., ROISENBERG, I. & SCHULER-FACCINI, L. 2009. Evaluation of C677T and A1298C polymorphisms of the MTHFR gene as maternal risk factors for Down syndrome and congenital heart defects. *Am J Med Genet A,* 149A**,** 2080-7.

CHARTIER, A., ZAFFRAN, S., ASTIER, M., SEMERIVA, M. & GRATECOS, D. 2002. Pericardin, a Drosophila type IV collagen-like protein is involved in the morphogenesis and maintenance of the heart epithelium during dorsal ectoderm closure. *Development,* 129**,** 3241-53.

CHEN, M. Y., RIEHLE-COLARUSSO, T., YEUNG, L. F., SMITH, C., EDS & FARR, S. L. 2018. Children with Heart Conditions and Their Special Health Care Needs - United States, 2016. *MMWR Morb Mortal Wkly Rep,* 67**,** 1045-1049.

CHO, J., HUR, J. H., GRANIEL, J., BENZER, S. & WALKER, D. W. 2012. Expression of yeast NDI1 rescues a Drosophila complex I assembly defect. *PLoS One,* 7**,** e50644.

COFFMAN, J. A. & DAVIDSON, E. H. 2001. Oral-aboral axis specification in the sea urchin embryo. I. Axis entrainment by respiratory asymmetry. *Dev Biol,* 230**,** 18-28.

CUCORANU, I., CLEMPUS, R., DIKALOVA, A., PHELAN, P. J., ARIYAN, S., DIKALOV, S. & SORESCU, D. 2005. NAD(P)H oxidase 4 mediates transforming growth factor-beta1-induced differentiation of cardiac fibroblasts into myofibroblasts. *Circ Res,* 97**,** 900-7.

DIKALOVA, A. E., BIKINEYEVA, A. T., BUDZYN, K., NAZAREWICZ, R. R., MCCANN, L., LEWIS, W., HARRISON, D. G. & DIKALOV, S. I. 2010. Therapeutic targeting of mitochondrial superoxide in hypertension. *Circ Res,* 107**,** 106-16.

FOLMES, C. D., DZEJA, P. P., NELSON, T. J. & TERZIC, A. 2012. Mitochondria in control of cell fate. *Circ Res,* 110**,** 526-9.

FUKAI, T. & USHIO-FUKAI, M. 2011. Superoxide dismutases: role in redox signaling, vascular function, and diseases. *Antioxid Redox Signal,* 15**,** 1583-606.

GAJEWSKI, K., CHOI, C. Y., KIM, Y. & SCHULZ, R. A. 2000. Genetically distinct cardial cells within the Drosophila heart. *Genesis,* 28**,** 36-43.

GARCIA-DIAZ, L., COSERRIA, F. & ANTINOLO, G. 2013. Hypertrophic Cardiomyopathy due to Mitochondrial Disease: Prenatal Diagnosis, Management, and Outcome. *Case Rep Obstet Gynecol,* 2013**,** 472356.

GILBOA, S. M., DEVINE, O. J., KUCIK, J. E., OSTER, M. E., RIEHLE-COLARUSSO, T., NEMBHARD, W. N., XU, P., CORREA, A., JENKINS, K. & MARELLI, A. J. 2016. Congenital Heart Defects in the United States: Estimating the Magnitude of the Affected Population in 2010. *Circulation,* 134**,** 101-9.

GIORDANO, F. J. 2005. Oxygen, oxidative stress, hypoxia, and heart failure. *J Clin Invest,* 115**,** 500-8.

GIORGIO, M., TRINEI, M., MIGLIACCIO, E. & PELICCI, P. G. 2007. Hydrogen peroxide: a metabolic by-product or a common mediator of ageing signals? *Nat Rev Mol Cell Biol,* 8**,** 722-8.

GRIGORIAN, M., MANDAL, L., HAKIMI, M., ORTIZ, I. & HARTENSTEIN, V. 2011. The convergence of Notch and MAPK signaling specifies the blood progenitor fate in the Drosophila mesoderm. *Dev Biol,* 353**,** 105-18.

HOFFMAN, J. I. & KAPLAN, S. 2002. The incidence of congenital heart disease. *J Am Coll Cardiol,* 39**,** 1890-900.

ITANI, H. A., DIKALOVA, A. E., MCMASTER, W. G., NAZAREWICZ, R. R., BIKINEYEVA, A. T., HARRISON, D. G. & DIKALOV, S. I. 2016. Mitochondrial Cyclophilin D in Vascular Oxidative Stress and Hypertension. *Hypertension,* 67**,** 1218-27.

IWANAGA, Y., AOYAMA, T., KIHARA, Y., ONOZAWA, Y., YONEDA, T. & SASAYAMA, S. 2002. Excessive activation of matrix metalloproteinases coincides with left ventricular remodeling during transition from hypertrophy to heart failure in hypertensive rats. *J Am Coll Cardiol,* 39**,** 1384-91.

KARAMANLIDIS, G., NASCIMBEN, L., COUPER, G. S., SHEKAR, P. S., DEL MONTE, F. & TIAN, R. 2010. Defective DNA replication impairs mitochondrial biogenesis in human failing hearts. *Circ Res,* 106**,** 1541-8.

KHAN, R. & SHEPPARD, R. 2006. Fibrosis in heart disease: understanding the role of transforming growth factor-beta in cardiomyopathy, valvular disease and arrhythmia. *Immunology,* 118**,** 10-24.

LEPTIN, M. 1991. twist and snail as positive and negative regulators during Drosophila mesoderm development. *Genes Dev,* 5**,** 1568-76.

LIOCHEV, S. I. 2013. Reactive oxygen species and the free radical theory of aging. *Free Radic Biol Med,* 60**,** 1-4.

LO, P. C. & FRASCH, M. 2001. A role for the COUP-TF-related gene seven-up in the diversification of cardioblast identities in the dorsal vessel of Drosophila. *Mech Dev,* 104**,** 49-60.

LOEFFEN, J., ELPELEG, O., SMEITINK, J., SMEETS, R., STOCKLER-IPSIROGLU, S., MANDEL, H., SENGERS, R., TRIJBELS, F. & VAN DEN HEUVEL, L. 2001. Mutations in the complex I NDUFS2 gene of patients with cardiomyopathy and encephalomyopathy. *Ann Neurol,* 49**,** 195-201.

LOEFFEN, J. L., SMEITINK, J. A., TRIJBELS, J. M., JANSSEN, A. J., TRIEPELS, R. H., SENGERS, R. C. & VAN DEN HEUVEL, L. P. 2000. Isolated complex I deficiency in children: clinical, biochemical and genetic aspects. *Hum Mutat,* 15**,** 123-34.

MARIN-GARCIA, J., ANANTHAKRISHNAN, R., GOLDENTHAL, M. J., FILIANO, J. J. & PEREZ-ATAYDE, A. 1997. Cardiac mitochondrial dysfunction and DNA depletion in children with hypertrophic cardiomyopathy. *J Inherit Metab Dis,* 20**,** 674-80.

MATSUZAWA, A. & ICHIJO, H. 2005. Stress-responsive protein kinases in redox-regulated apoptosis signaling. *Antioxid Redox Signal,* 7**,** 472-81.

MEDIONI, C., ASTIER, M., ZMOJDZIAN, M., JAGLA, K. & SEMERIVA, M. 2008. Genetic control of cell morphogenesis during Drosophila melanogaster cardiac tube formation. *J Cell Biol,* 182**,** 249-61.

MURDOCH, C. E., ZHANG, M., CAVE, A. C. & SHAH, A. M. 2006. NADPH oxidase-dependent redox signalling in cardiac hypertrophy, remodelling and failure. *Cardiovasc Res,* 71**,** 208-15.

NA, J., MUSSELMAN, L. P., PENDSE, J., BARANSKI, T. J., BODMER, R., OCORR, K. & CAGAN, R. 2013. A Drosophila model of high sugar diet-induced cardiomyopathy. *PLoS Genet,* 9**,** e1003175.

NEUBAUER, S. 2007. The failing heart--an engine out of fuel. *N Engl J Med,* 356**,** 1140-51.

NISHIOKA, K., VILARINO-GUELL, C., COBB, S. A., KACHERGUS, J. M., ROSS, O. A., HENTATI, E., HENTATI, F. & FARRER, M. J. 2010. Genetic variation of the mitochondrial complex I subunit NDUFV2 and Parkinson's disease. *Parkinsonism Relat Disord,* 16**,** 686-7.

OCORR, K., FINK, M., CAMMARATO, A., BERNSTEIN, S. & BODMER, R. 2009. Semi-automated Optical Heartbeat Analysis of small hearts. *J Vis Exp.*

PETERSON, C., AILES, E., RIEHLE-COLARUSSO, T., OSTER, M. E., OLNEY, R. S., CASSELL, C. H., FIXLER, D. E., CARMICHAEL, S. L., SHAW, G. M. & GILBOA, S. M. 2014. Late detection of critical congenital heart disease among US infants: estimation of the potential impact of proposed universal screening using pulse oximetry. *JAMA Pediatr,* 168**,** 361-70.

PIAZZA, N. & WESSELLS, R. J. 2011. Drosophila models of cardiac disease. *Prog Mol Biol Transl Sci,* 100**,** 155-210.

PURNOMO, Y., PICCART, Y., COENEN, T., PRIHADI, J. S. & LIJNEN, P. J. 2013. Oxidative stress and transforming growth factor-beta1-induced cardiac fibrosis. *Cardiovasc Hematol Disord Drug Targets,* 13**,** 165-72.

RHEE, S. G. 2006. Cell signaling. H2O2, a necessary evil for cell signaling. *Science,* 312**,** 1882-3.

ROBINSON, C. M., NEARY, R., LEVENDALE, A., WATSON, C. J. & BAUGH, J. A. 2012. Hypoxia-induced DNA hypermethylation in human pulmonary fibroblasts is associated with Thy-1 promoter methylation and the development of a pro-fibrotic phenotype. *Respir Res,* 13**,** 74.

SCHEUBEL, R. J., TOSTLEBE, M., SIMM, A., ROHRBACH, S., PRONDZINSKY, R., GELLERICH, F. N., SILBER, R. E. & HOLTZ, J. 2002. Dysfunction of mitochondrial respiratory chain complex I in human failing myocardium is not due to disturbed mitochondrial gene expression. *J Am Coll Cardiol,* 40**,** 2174-81.

SENA, L. A. & CHANDEL, N. S. 2012. Physiological roles of mitochondrial reactive oxygen species. *Mol Cell,* 48**,** 158-67.

SYKIOTIS, G. P. & BOHMANN, D. 2008. Keap1/Nrf2 signaling regulates oxidative stress tolerance and lifespan in Drosophila. *Dev Cell,* 14**,** 76-85.

TAO, Y. & SCHULZ, R. A. 2007. Heart development in Drosophila. *Semin Cell Dev Biol,* 18**,** 3-15.

TSAI, S., KUIT, V., LIN, Z. G. & LIN, C. 2014. Application of a functional marker for the effect of cryoprotectant agents on gorgonian coral (Junceella juncea and J. fragilis) sperm sacs. *Cryo Letters,* 35**,** 1-7.

VERKLEIJ-HAGOORT, A. C., VERLINDE, M., URSEM, N. T., LINDEMANS, J., HELBING, W. A., OTTENKAMP, J., SIEBEL, F. M., GITTENBERGER-DE GROOT, A. C., DE JONGE, R., BARTELINGS, M. M., STEEGERS, E. A. & STEEGERS-THEUNISSEN, R. P. 2006. Maternal hyperhomocysteinaemia is a risk factor for congenital heart disease. *BJOG,* 113**,** 1412-8.

WANG, B., LIU, M., YAN, W., MAO, J., JIANG, D., LI, H. & CHEN, Y. 2013. Association of SNPs in genes involved in folate metabolism with the risk of congenital heart disease. *J Matern Fetal Neonatal Med,* 26**,** 1768-77.

WANG, J., HOSHIJIMA, M., LAM, J., ZHOU, Z., JOKIEL, A., DALTON, N. D., HULTENBY, K., RUIZ-LOZANO, P., ROSS, J., JR., TRYGGVASON, K. & CHIEN, K. R. 2006. Cardiomyopathy associated with microcirculation dysfunction in laminin alpha4 chain-deficient mice. *J Biol Chem,* 281**,** 213-20.

WARD, E. J. & SKEATH, J. B. 2000. Characterization of a novel subset of cardiac cells and their progenitors in the Drosophila embryo. *Development,* 127**,** 4959-69.

WEBER, K. T. & BRILLA, C. G. 1991. Pathological hypertrophy and cardiac interstitium. Fibrosis and renin-angiotensin-aldosterone system. *Circulation,* 83**,** 1849-65.

WEBER, K. T., SUN, Y., TYAGI, S. C. & CLEUTJENS, J. P. 1994. Collagen network of the myocardium: function, structural remodeling and regulatory mechanisms. *J Mol Cell Cardiol,* 26**,** 279-92.

WENINK, A. C. & GITTENBERGER-DE GROOT, A. C. 2005. Pathogenesis of congenital cardiac malformations and mechanisms of cardiac remodelling. *Cardiol Young,* 15 Suppl 3**,** 3-6.

WOJTOVICH, A. P., BERRY, B. J. & GALKIN, A. 2019. Redox Signaling Through Compartmentalization of Reactive Oxygen Species: Implications for Health and Disease. *Antioxid Redox Signal,* 31**,** 591-593.

ZAFFRAN, S., REIM, I., QIAN, L., LO, P. C., BODMER, R. & FRASCH, M. 2006. Cardioblast-intrinsic Tinman activity controls proper diversification and differentiation of myocardial cells in Drosophila. *Development,* 133**,** 4073-83.

ZHANG, H., GOMEZ, A. M., WANG, X., YAN, Y., ZHENG, M. & CHENG, H. 2013. ROS regulation of microdomain Ca(2+) signalling at the dyads. *Cardiovasc Res,* 98**,** 248-58.

ZIELONKA, J., SRINIVASAN, S., HARDY, M., OUARI, O., LOPEZ, M., VASQUEZ-VIVAR, J., AVADHANI, N. G. & KALYANARAMAN, B. 2008. Cytochrome c-mediated oxidation of hydroethidine and mito-hydroethidine in mitochondria: identification of homo- and heterodimers. *Free Radic Biol Med,* 44**,** 835-46.